27
7/15/80 T.S.

SAND79-2226
Unlimited Release
UC 70

MASTER

Salt Block II: Description and Results

Jacque J. Hohlfelder

SF 2900-Q(3-80)

UC-70

SAND79-2226
Unlimited Release

SALT BLOCK II: DESCRIPTION AND RESULTS

J. J. Hohlfelder
Division 1112
Sandia National Laboratories
Albuquerque, New Mexico 87185

ABSTRACT

A description of and results from the Salt Block II experiment, which involved the heating of and measurement of water transport within a large sample of rock salt, are presented. These results include the measurement of water released into a heated borehole in the sample as well as measured temperatures within the salt. Measured temperatures are compared with the results of a mathematical model of the experiment.

DISCLAIMER

This book was prepared as an account of work sponsored by an agency of the United States Government. Neither the United States Government nor any agency thereof, nor any of their employees, makes any warranty, express or implied, or assumes any legal liability or responsibility for the accuracy, completeness, or usefulness of any information, apparatus, product, or process disclosed, or represents that its use would not infringe privately owned rights. Reference herein to any specific commercial product, process, or service by trade name, trademark, manufacturer, or otherwise, does not necessarily constitute or imply its endorsement, recommendation, or favoring by the United States Government or any agency thereof. The views and opinions of authors expressed herein do not necessarily state or reflect those of the United States Government or any agency thereof.

DISTRIBUTION OF THIS DOCUMENT IS UNLIMITED

ACKNOWLEDGMENTS

The persistent hard work of many individuals contributed to the successful performance of this experiment. The assistance of the following persons is gratefully acknowledged: Jay Benson (deceased), Richard Baff (1124), Austin Arthur (1125), James Johnson (1125), John Loukota (1125), James McIlmoyle (1125), Frank Dean (1761), Stephen Breeze (2452), John Stott (retired), Henry Shefelbine (4541), Allan Sattler (4732), Ramon Villegas (4733), and Oscar George (5511).

PREFACE

This document is a description of the Salt Block II experiment and a summary of the experiment's major events. It presents a complete, though tentative, summary of the experiment's water transport data as well as sufficient thermal data to enable detailed, quantitative water transport modeling.

INTRODUCTION

The Salt Block II experiment was a laboratory experiment involving the heating of and measurement of water transport within a large specimen of bedded geologic salt. The two principal technical objectives of the test were:

1. The quantitative, time-dependent, redundant measurement of the water released into a heated borehole in a large (2 ton) sample of rocksalt.

2. The measurement of temperatures and of heat flux at selected locations within the salt sample, its heater, and its enclosure. The purpose of these measurements is to provide for a comparison with the predictions of a mathematical model of this experiment.

The release of water into a heated borehole is of interest because arguments have been advanced, which state that this phenomenon could degrade the ability of a nuclear waste repository in bedded salt to isolate radionuclides from the biosphere. Since this transport of water (including the phenomenon, "brine-migration") may be governed by both temperature and temperature gradient, accurate knowledge of these parameters within the salt block are essential.

EXPERIMENT DESCRIPTION

The experiment consisted of a 1-meter-diameter by 1-meter-high cylindrical block of rocksalt with a borehole 0.13-meters diameter by 0.8-meters deep on its axis for an electrical heater. The block was placed inside a gas-tight stainless steel container whose outside circumference was cooled with a water jacket. The thermal field within the block was measured with thermocouples and heat flux gages that were installed on the electrical heater, within the salt block, and on its outside surface. Water release from the heated borehole was measured by continuously purging the sealed borehole with very dry nitrogen gas and measuring the water content in the

exhaust gas with two independent techniques. Data were automatically recorded by a computer-based data acquisition system.

A simplified schematic and a photograph of the assembled experiment are shown in Figures 1 and 2. The major components of the experiment were the salt block, the heater and water jacket systems, the temperature sensors, the moisture measurement system and the data acquisition system, all of which are described below.

Salt Block

The salt block (Figure 3) was machined from a large block of bedded salt obtained from the Mississippi Chemical Company's potash mine in southeastern New Mexico. The total volatile content, most of which is water, of this salt ranges between 0.1 and 0.5 percent by weight. Both the mineralogy of the salt block and its stress state may be different from the in situ conditions at the proposed WIPP horizons; therefore, the water release rates measured in this experiment may be different from those in the WIPP facility.

Heater and Water Jacket System

The thermal environment in the block was determined by the electrical heater along its axis and by the controlled thermal boundary conditions of the salt block's enclosure. The boundary conditions were defined by a water cooling jacket around the circumference and by thermal insulation on the top and bottom of the block. At the maximum heater power of 1.5 kilowatts, the maximum temperature and temperature gradient at the surface of the heater hole were about 200°C and 12°C/cm, respectively.

Temperature Measurement

The thermal field in the salt block was measured and predicted theoretically as a function of time and position (both axially and radially). The experiment was instrumented with approximately 40 thermocouples and 10 heat flux gages. A two-dimensional, finite-difference model was used to predict the time-dependent temperatures within the block. For the most part the parameters used in the model were either known materials properties or measured boundary condition values. However, the temperature-dependent thermal conductivity of the salt was adjusted so that measured temperatures matched the calculated ones.

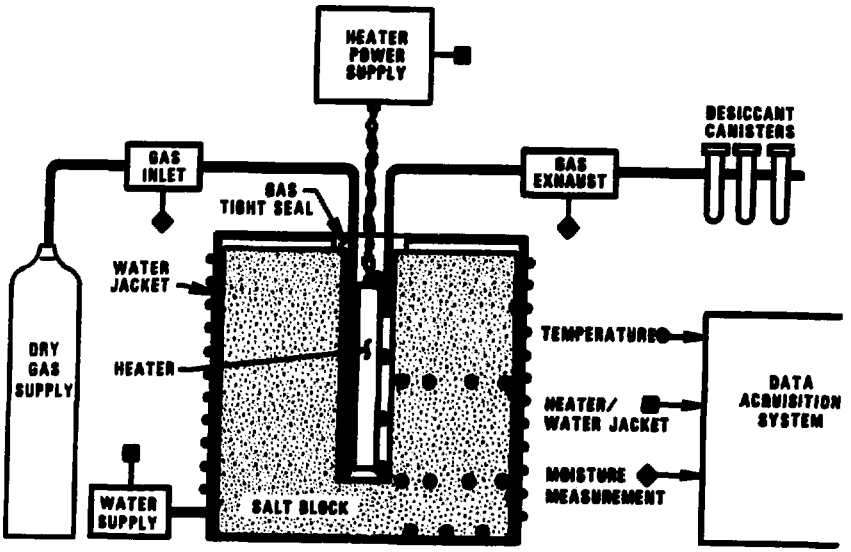

Figure 1. SCHEMATIC OF THE SALT BLOCK II EXPERIMENT

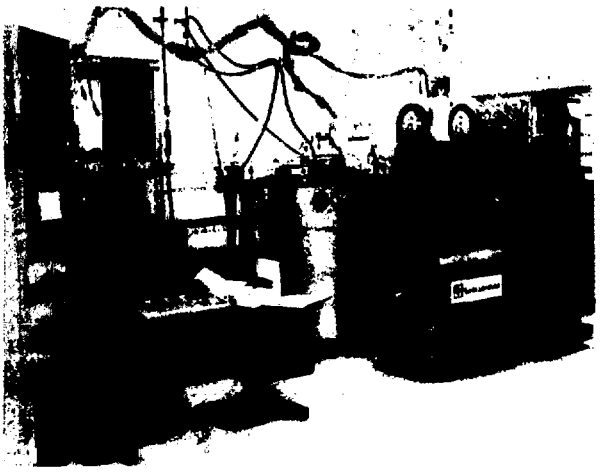

Figure 2. ASSEMBLED SALT BLOCK II EXPERIMENT

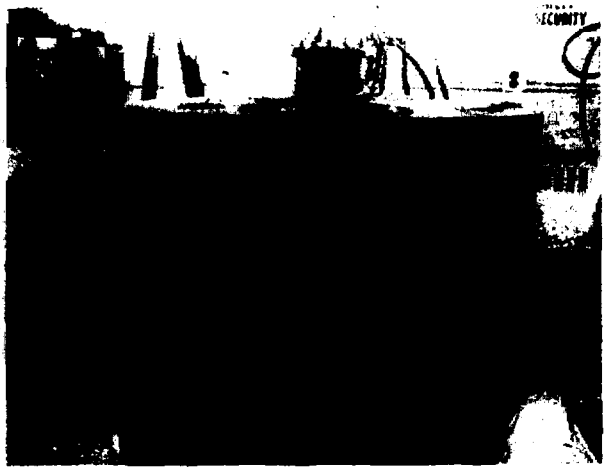

Figure 3. SALT BLOCK II PRIOR TO PLACEMENT IN ENCLOSURE

Moisture Collection System

As shown in Figure 1, any moisture released in the heater hole was removed by purging the annular volume between the heater can and the heater hole with very dry nitrogen gas. The amount of water in the purge gas was determined by two techniques:

1) The temperature, pressure, dew point and flow rate of the purge gas (both inlet and exhaust) were measured and used to calculate the rate at which water was being extracted from the salt. The rate was integrated to yield the cumulative water release.

2) The purge gas exhaust was passed through water-specific, desiccant canisters. These canisters were changed periodically and accurately weighed before and after use. The weight gain of the canisters was taken to be the amount of water in the purge gas.

These two techniques for measuring water loss were evaluated, and they proved to be consistent within about 10 percent in a series of experiments on small rocksalt samples.[1]

Data Acquisition System

Data from the 120 channels of diagnostic instrumentation generated during the course of the experiment were automatically recorded by a computer-based data-acquisition system. This system sampled the sensors at specified intervals, digitized the outputs, converted them to engineering units, and then calculated the rate of moisture release from the measured pressure, temperature, dew point and flow-rate data.

EVENT SUMMARY

A discussion of the experiment's major events is presented here. Some of these were unexpected, but in general, water transport measurements and thermal field measurements continued uninterrupted until the experiment's conclusion.

The experiment began November 28, 1978. After six days, heater power was applied and increased in discrete steps through January 3, 1979, at which time the power was increased from 0.6 kW to 1.0 kW.

On January 9, an unexpected power outage resulted in the loss of electrical power to the experiment's heater. The outage lasted about 30 minutes. Water cooling of the salt block's enclosure continued, and temperatures of the salt block and heater declined.

The 1.5 kW heating phase began on Janaury 16. On January 24, a broken water main caused a loss of the experiment's cooling water for about 16 hours. The maximum temperature increase in the salt block, which occurred near its top surface, was about 20°C.

During the remainder of the 1.5 kW heating phase, several gages became inoperative or unreliable, although no significant data were lost due to these gage failures. The water flow rate gages and several heat flux gages failed. The dew point gages became less reliable because of frequent fouling. After February 19, only the desiccant canister method was used to measure water evolved into the borehole region. Both the heater current and voltage were measured, and the heater power was calculated from these quantities. A slow increase in the temperatures within the salt was observed; this was caused in part by the rise in the temperature of the cooling water from its winter minimum.

The shutdown phase began on March 26, 1979, and consisted of three, sequential heater power reductions. Heater power was reduced from 1.5 kW to 1.0 kW, from 1.0 kW to 0.6 kW, and from 0.6 kW to 0 kW. Following each heater power reduction, the experiment continued at constant heater power for approximately one week.

Following each of the heater power reductions occurring during the shutdown phase, transient and relatively large water inflow rates were measured. This phenomenon was expected, based upon earlier measurements of water lost from heated 1 kg salt samples. Water lost during the shutdown phase accounted for a large fraction (43 percent) of the water measured during the course of the experiment.

At the end of the shutdown phase, the measurements of water evolved into the heater region were terminated, and the experiment's disassembly was started April 16, 1979. The dissassembly phase (including the end of all active sensor recording, removal of the experiment's cover and shell, and evaluation of the effects of the experiment on the salt block, the heater, and the seals) lasted two days.

Following removal of water-cooling lines, electrical leads, and gas-flow plumbing, the experiment disassembly continued with the removal of the leak seal material from the top of the heater, and the removal of the gas seal bellows, the experiment cover, and the cylindrical shell. Little evidence of water or water transport in the region between the cylindrical shell and the salt block was present. Approximately 1 g of water remained as condensate--primarily on the periphery of the bottom plate. Traces of corrosion were present on the stainless steel experimental materials. Visible evidence of fluid transport occurred only as thin salt crusts in isolated regions around the outer surface of the salt block, but occurred more generally on the inner surface of the salt block in the region surrounding the heater. Removal of the crushed salt backfill from around the heater and the removal of the heater was simple. Essentially all of the backfill material was recovered. The heater was lifted from the borehole and showed very little corrosion; no borehole deformation or cementing of the heater with brine encrustation was evident. Some cracking and separation of the salt block along its horizontal bedding planes occurred, but these cracks were limited to approximately the middle one-third of the block (i.e., the 0.3 m thick, cylindrical section located symmetrically about the block's horizontal midplane) and did not extend into the region surrounding the heater. Despite the occurrence of this cracking within the salt, the salt was sufficiently intact so that the salt block could be lifted by the seal at its top surface. No cracking between thermocouple boreholes occurred, and the seals in these holes appeared unaltered. The elastomeric gas seal between the heater collar and the salt block was not only intact, but its adhesive bond was sufficient to support the mass of the salt block. In general, the heat flux gage adhesive bonds remained intact, including those bonded to the surface of the heater.

Following experiment disassembly, post-test sampling of the salt block continued intermittently until about July 1. Removal of material samples from the salt block was a protracted operation lasting two months. In order to remove samples from a region within the block that had experienced large temperature changes, a one-foot-thick cylindrical slab was hand sawn from the top of the salt block. Salt samples were removed from the material exposed on this "freshly" cut surface. Additionally, around June 25, four

4-inch-diameter vertically oriented cores were removed from the material below the freshly cut surface. The core centers were at varying radial distances from the axis of the salt block. Specimens from both sets of salt samples were examined for water content.

The experimental events are listed here in chronological order:

Date	Event Description
November 28, 1978:	The experiment was started (water transport measurements), but with no heater power.
December 4, 1978:	Heater power was turned on at a level of 0.2 kW.
December 11, 1978:	Heater power was raised from 0.2 kW to 0.4 kW.
December 18, 1978:	Heater power was raised from 0.4 kW to 0.6 kW.
January 2, 1979:	Heater power was raised from 0.6 kW to 1.0 kW.
January 8, 1979:	Power outage (approximately 0.5 hour).
January 16, 1979:	Heater power was raised from 1.0 kW to 1.5 kW.
January 24, 1979:	Water jacket cooling interruption.
March 26, 1979:	Shutdown phase started; heater power reduced from 1.5 kW to 1.0 kW.
April 2, 1979:	Heater power reduced from 1.0 kW to 0.6 kW.
April 9, 1979:	Heater power turned off.
April 16, 1979:	The experiment was turned off (water transport measurements terminated).
April 16-30, 1979:	The experiment was disassembled and inspected.
May-June, 1979:	Post-test samples from the salt block were obtained.

RESULTS

Both of the experimental objectives outlined in the introduction have been met, and water transport measurement and thermal behavior results are presented below.

WATER TRANSPORT MEASUREMENTS

A summary of the major results for each heating phase of the Salt Block II experiment, including thermal and water loss data, is shown in Table I. Only 111.4 gm of water was released during the approximately 140-day-long experiment. A major fraction of the water evolved (45 percent) was released during the 10-week long, 1.5 kW heater power phase; however, 43 percent of the water was released during the three-week-long shutdown phase. The greatest water release rates were observed following heater power decreases. Although the maximum thermal gradient at the heater borehole surface is tabulated, nothing in the results indicate that this is a significant parameter in understanding water transport in salt on this physical scale. The absolute value of the radial component of calculated values of the equilibrium thermal gradient within the salt block are presented in the section, "THERMAL BEHAVIOR." As indicated in the last column of Table I, a relatively high average rate of water release occurs in the first two days following any change in the heater power; this is most pronounced in two instances in which the heater power was reduced.

A more detailed summary of the water mass loss measurements is presented in Table II. The table lists water mass loss results determined by each of two independent methods. Time-dependent mass loss rates were calculated from the measurement of the dew point and gas flow parameters (volume flow rate, absolute pressure, and temperature) of the nitrogen gas stream which scavenged water from the region between the borehole and the heater. The integral of the water mass loss rate yielded the total mass of water lost over the integral's time interval. Shown in Table II are values of this integral evaluated from times identical to those at which desiccant canister measurements of water mass were made. The errors reported for the mass rate

TABLE I

SUMMARY OF THERMAL AND WATER LOSS RESULTS

EVENT DESCRIPTION AND NOMINAL HEATER POWER	EVENT TIME DAYS OR DAY OF YEAR	MEASURED HEATER POWER kW		TEMPERATURE TC @11 °C	TEMPERATURE HEATER SURFACE °C	CALCULATED TEMPERATURE OF HEATER SURFACE °C	CALCULATED THERMAL CONDUCTANCE °C.cm^{-1}
		Preceding Event	Following Event				
			b	c	d	e	f
Experiment starts. Heater pwr at 0.1W	331.969	0.0	0.0	10.3	10.4	---	0
Heater pwr raised--0 to 0.2 kW	337.008	0.0	0.197	35.5	52.3	30	-1.2
Heater pwr raised--0.2kW to 0.4kW	344.461	0.195	0.396	53.3	84.0	50	-2.5
Heater pwr raised from 0.4kW to 0.6kW	351.486	0.396	0.595	72.3	115.6	81	-4.1
Heater pwr raised from 0.6kW to 1.0kW	1.470	0.591	1.000	113.5	183.8	130	-7.6
Power outage (40 min maximum)	8.481	1.000	0	100.4	125.2	---	---
Resumption of heater power	8.500	0	1.000	---	---	---	---
Heater pwr raised from 1.0kW to 1.9kW	15.544	1.000	1.907	171.1[3] 176.1	275.0[3] 281.3	198, 204[3]	-12.7[3] -13.0
Intermittent loss/cooling water	23.604	1.525	1.525	191.3	302.3	---	---
Resumption of coolant flow	24.371	1.525	1.525	---	---	---	---
Powered shutdown, heater pwr lowered from 1.9kW to 1.0kW	84.414	1.525	1.000	121.1	193.1	138	-7.9
Powered shutdown, heater pwr lowered from 1.0kW to 0.6kW	91.394	1.000	0.602	80.3	126.1	90	-4.5
Powered shutdown, heater pwr turned off	97.601	0.602	0	19.4	19.4	19.4	0
Experiment recording terminated, disassembly started	105.342	---	---	---	---	---	---

TABLE I (CONTINUED)
SUMMARY OF THERMAL AND WATER LOSS RESULTS

EVENT DESCRIPTION AND NOMINAL HEATER POWER	$gm.min^{-1}$ WATER EVOLUTION RATE: Prior to Event	$gm.min^{-1}$ WATER EVOLUTION RATE: Maximum Following Event	WATER EVOLVED, 2-day Interval gm	WATER EVOLVED BETWEEN EVENTS gm	CUMULATIVE WATER EVOLVED, FROM START TO NEXT EVENT	TIME BETWEEN EVENTS - DAYS	RATIO: WATER EVOLUTION RATE 2-DAY/EVENT INTERVAL
	a		g	h			
Experiment starts. Heater pwr at 0.1W	—	8.21×10^{-5}	.124 ± .023	.273 ± .049	.273 ± .049	5.98	1.4
Heater pwr raised—0 to 0.2 W	1.58×10^{-5}	9.55×10^{-5}	.178 ± .061	.406	.799	6.99	1.3
Heater pwr raised—0.2W to 0.4W	2.21×10^{-5}	9.63×10^{-5}	.193 ± .092	.559	.132	7.03	1.2
Heater pwr raised from 0.4W to 0.6W	2.90×10^{-5}	1.53×10^{-4}	.279 ± .155	1.21	2.52	10.90	1.7
Heater pwr raised from 0.6W to 1.0W	2.11×10^{-5}	1.36×10^{-3}	2.04 ± .73	10.69	13.21	14.07	1.3
Power outage (40 min maximum)	2.14×10^{-4}	1.38×10^{-2}	6.78 ± 1.57	10.69	13.21	14.07	3.2
Resumption of heater power	—	—	—	—	—	—	—
Heater pwr raised from 1.0W to 1.5W	1.86×10^{-4}	6.73×10^{-3}	3.32 ± 2.12	49.97	63.18	68.87	2.3
Intermittent loss/cooling water	6.16×10^{-4}	1.82×10^{-3}	2.98 ± 1.90	49.97	63.18	68.87	2.1
Resumption of coolant flow	—	—	—	—	—	—	—
Powered shutdown, heater pwr lowered from 1.5W to 1.0W	3.0×10^{-4}	1.77×10^{-2}	22.6	29.98	92.26	6.98	2.6
Powered shutdown, heater pwr lowered from 1.0W to 0.6W	8.0×10^{-4}	3.10×10^{-3}	5.30	13.40	105.66	7.01	1.4
Powered shutdown, heater pwr turned off	1.06×10^{-3}	1.40×10^{-3}	2.64	5.77	111.42	6.94	1.6
Experiment recording terminated, disassembly started	—	—	—	—	—	—	—

TABLE I (CONTINUED)
SUMMARY OF THERMAL AND WATER LOSS RESULTS

NOTES

a Systematic errors in the Panametrics dew-point gage data have been corrected. Data taken with the chilled-mirror dew-point gages were not used in calculations of water loss rates during periods in which the mirrors were fouled.

b Heater powers are calculated from the measured heater voltages and currents.

c The location of thermocouple 11 (TC #11) within the salt block is approximately 16.8 cm radially outward from the block's axis of symmetry, along the midplane of the block. The highest observed salt block temperatures were measured on this gage. The temperatures listed here are equilibrium temperatures that are reached approximately three days following changes in heater power or boundary temperatures.

d The maximum temperature measured on the surface of the heater by either thermocouple 5 (at low heater power levels) or thermocouple 6 (at high heater power levels) is shown in this column.

e This temperature is calculated for a position along the midplane of the salt block, 2.5 cm radially inward from TC #11. This is at the surface of the heater borehole adjacent to the crushed salt backfill. The calculation assumes cylindrical symmetry and no axial component of heat flux; it simply extrapolates the TC #11 temperature radially inward.

f The thermal gradient is calculated at the position of the temperatures in column six. Note that this is an estimate of the maximum gradient expected on the borehole surface and that the thermal gradient over most of the borehole surface is much smaller.

g The water evolved is determined using the dew-point gage data (except for the last three entries). The interval begins with the time of the event noted and lasts for two days.

h The water evolved is determined using the desiccant canister method (except for the first entry). The interval begins with the time of the event noted in the first column and concludes with the time of the next event listed in the first column.

i The water loss rate following the approximately 40-minute heater power failure on January 9 exceeded the measured rate listed. The measured rate reflects the fact that the gas flow system output leg became saturated with respect to water at room temperature.

j The two values listed for the 1.5 kW heating phase refer to temperatures or heat fluxes determined at the beginning and at the end of the phase, respectively. The increase in these quantities with time is due, in part, to the increase in the average coolant temperature as well as the decrease in the salt's thermal conductivity.

TABLE II

WATER MASS LOSS MEASUREMENTS FROM SALT BLOCK II EXPERIMENT

EVENT TIME	DATE	TIME FROM EXPERIMENT START	NOMINAL REACTOR POWER	WATER LOSS MEASUREMENT METHOD: HEAT BALANCE CALCULATED — Interval $\sum_{c}^{H} \pm \Delta \sum_{c}^{H}$	HEAT BALANCE CALCULATED — Cumulative $\left\{\sum_{c}^{H} \pm \Delta \sum_{c}^{H}\right\}$	MASS FLOW RATE INTEGRALS — Interval $\int_{t_{i-1}}^{t_i} \dot{M} dt \pm \Delta \int_{t_{i-1}}^{t_i} \dot{M} dt$	MASS FLOW RATE INTEGRALS — Cumulative $\int_{0}^{t_i} \dot{M} dt \pm \Delta \int_{0}^{t_i} \dot{M} dt$	TOTAL WATER FOR POWER PERIOD
HRMET	HYDP	DAYS	MW	gm	gm	gm	gm	gm
331.569	(330.000)	(0.000)	0	—	—	.273 ± .049	.273 ± .049	.273 ± .049
-	344.391	12.822	0.2	.7585 ± .0002	.7585 ± .0002	.70 ± .12	.70 ± .12	.7585 ± .0002
344.391	351.470	19.900	0.4	.5573 ± .0003	1.3158 ± .0004	.50 ± .17	1.20 ± .21	.5573 ± .0003
351.478	1.362	34.793	0.6	1.207 ± .003	2.523 ± .003	1.16 ± .44	2.36 ± .48	1.207 ± .003
1.362	7.458	40.889	1.0	4.046 ± .003	6.569 ± .004	3.86 ± 1.11	6.22 ± 1.21	4.046 ± .003
7.458	8.587	42.010	1.0	7.094 ± .0006	7.278 ± .004	.97 ± .52	6.79 ± 1.32	4.755 ± .003
8.587	9.606	42.037	1.0	3.565 ± .005	10.823 ± .007	4.06 ± 1.41	10.83 ± 1.93	8.300 ± .006
9.606	15.528	48.959	1.0	2.330 ± .013	13.211 ± .015	2.11 ± 1.92	12.9 ± 2.9	10.000 ± .014
15.538	21.292	54.723	1.5	11.06 ± .13	24.27 ± .13	7.12 ± 3.14	20.1 ± 3.9	11.06 ± .13
21.292	28.394	61.825	1.5	7.810 ± .030	31.38 ± .13	6.19 ± 2.84	26.3 ± 4.8	18.07 ± .13
28.394	35.375	68.806	1.5	5.180 ± .016	36.46 ± .13	4.60 ± 2.75	30.9 ± 5.6	23.25 ± .13
35.375	42.385	75.816	1.5	4.437 ± .016	40.90 ± .14	3.62 ± 2.68	34.5 ± 6.2	27.69 ± .14
42.385	49.394	82.825	1.5	4.311 ± .026	45.21 ± .14	3.09 ± 3.05	37.6 ± 6.9	32.00 ± .14
49.394	56.353	89.784	1.5	3.951 ± .015	49.16 ± .14			35.95 ± .14

TABLE II (CONTINUED)

WATER MASS LOSS MEASUREMENTS FROM SALT BLOCK II EXPERIMENT

EVENT TIME		DATE		TIME FROM EXPERIMENT START	NOMINAL HEATER POWER	WATER LOSS MEASUREMENT METHOD				TOTAL WATER FOR POWER PHASE
						BALANCE CANISTER		STEAM FLOW RATE INTEGRALS		
						Interval	Cumulative	Interval	Cumulative	
						$\sum_c M \pm \Delta \sum_c M$	$\left\{\sum_c M \pm \Delta \sum_c M\right\}$	$\int_{t_{i-1}}^{t_i} \dot{M} dt \pm \Delta \int_{t_{i-1}}^{t_i} \dot{M} dt$	$\int_{s}^{t_i} \dot{M} dt \pm \Delta \int_{s}^{t_i} \dot{M} dt$	
START	STOP	DAYS	kW	gm		gm		gm		gm
56.353	63.350	96.789	1.5	3.730	± .007	52.90	± .14			39.69 ± .14
63.350	70.342	103.773	1.5	3.592	± .004	56.49	± .14			43.28 ± .14
70.342	77.358	110.789	1.5	3.521	± .002	60.01	± .14			46.80 ± .14
77.358	78.568	111.999	1.5	.5204	± .0007	60.53	± .14			47.32 ± .14
78.568	79.553	112.984	1.5	.0883	± .0019	60.62	± .14			47.41 ± .14
79.553	80.565	113.996	1.5	.7423	± .0005	61.36	± .14			48.15 ± .14
80.565	84.399	117.830	1.5	1.817	± .004	63.18	± .14			49.97 ± .14
84.399	84.550	117.981	1.0	2.300	± .008	65.48	± .14			2.300 ± .002
84.550	84.706	118.137	1.0	3.978	± .002	69.46	± .14			6.278 ± .003
84.706	85.286	118.717	1.0	12.221	± .037	81.68	± .14			18.50 ± .04
85.286	86.378	119.809	1.8	4.011	± .011	85.69	± .14			22.51 ± .04
86.378	88.363	121.794	1.0	3.078	± .004	88.77	± .14			25.59 ± .04
88.363	91.382	124.813	1.0	3.493	± .001	92.26	± .14			29.08 ± .04
91.382	91.529	124.960	0.6	.5484	± .0006	92.80	± .14			.5484 ± .0006

TABLE II (CONTINUED)

WATER MASS LOSS MEASUREMENTS FROM SALT BLOCK II EXPERIMENT

EVENT TIME		DAYS	TIME FROM EXPERIMENT START	NOMINAL REACTOR POWER	WATER LOSS MEASUREMENT METHOD				TOTAL WATER FOR POWER PHASE
					DENSITOMET CAPILLTER		MASS FLOW RATE INTEGRALS		
					Interval	Cumulative	Interval	Cumulative	
					$\sum_c M \pm \Delta \sum_c M$	$\left\{\sum_c M \pm \Delta \sum_c M\right\}$	$\int_{t_{i-1}}^{t_i} Mdt \pm \Delta \int_{t_{i-1}}^{t_i} Mdt$	$\int_{*}^{t_i} Mdt \pm \Delta \int_{*}^{t_i} Mdt$	
START	STOP	DAYS	MW	gm		gm	gm	gm	gm
91.529	91.706	125.137	0.6	.7089 ± .0005		93.59 ± .14			1.3293 ± .0008
91.706	92.384	125.815	0.6	2.22250 ± .0007		95.81 ± .14			3.554 ± .001
92.384	93.392	126.823	0.6	1.9815 ± .0019		97.80 ± .14			5.536 ± .002
93.392	95.354	128.785	0.6	3.2586 ± .0038		101.05 ± .14			8.796 ± .004
95.354	98.360	131.791	0.6	4.6082 ± .0052		105.66 ± .14			13.39 ± .01
98.360	98.532	131.963	0.0	.3368 ± .0052		105.99 ± .14			.3368 ± .0006
98.532	98.604	132.115	0.0	.3066 ± .0003		106.30 ± .14			.6435 ± .0007
98.604	99.350	132.781	0.0	1.1719 ± .0009		107.47 ± .14			1.8153 ± .0012
99.350	100.353	133.784	0.0	.8189 ± .0009		108.29 ± .14			2.634 ± .001
100.353	102.349	135.780	0.0	1.2839 ± .0007		109.57 ± .14			3.918 ± .002
102.349	105.342	138.773	0.0	1.8582 ± .0008		111.42 ± .14			5.768 ± .002

integrals are calculated from estimates of the uncertainties in the flow gas's measured dew points, absolute pressures, volume-flow rates and temperatures. The systematic error in the Panametrics brand dew point gage data has been corrected. The data taken with the chilled mirror dew point gages were not used in calculations of water mass loss rates during periods in which the mirrors were fouled.

Water loss measurements made using desiccant canisters to absorb water from the nitrogen flow gas stream are tabulated in Table II. For these water mass measurements, the error shown is due only to the estimated uncertainty arising from weighing the canisters. It includes no contributions which may arise from systematic incomplete or inadvertent water absorption. Figure 4 compares the sets of water mass loss results for the times up to February 19 in which both water mass measurement methods were used. In most instances, good agreement within the limits of error is shown.

That portion of the Salt Block II experiment of maximum duration at constant heater power was the 1.5 kW heating phase that lasted approximately 69 days. Except for the initial rise in the water mass loss rate, water release during this phase was characterized by a water mass loss rate declining monotonically to zero. Water mass loss data for this portion of the experiment together with the best power law functional form fit to 8 of 11 of these data is shown in Figure 5.

Nearly half of the water measured during the course of the experiment was measured during the three-week long heater power shutdown phase. At each of the three stages of this stepped reduction in heater power, a relatively large, time-dependent release of water was measured. In this regard, the behavior of the Salt Block II experiment was similar to that of heated, 1 kg samples of geologic salt that were measured earlier.[3]

One of the more striking features of the water transport measured during this experiment is its highly variable time-dependence. In general, significant, rapid changes in water mass loss rates were observed only after the heater power was changed. For each heater power change the numerically smoothed measured water mass loss rates for the six-day period following the heater power change are shown in Figures 6 through 15. The behavior of the water mass loss rate at the start of the experiment and following each

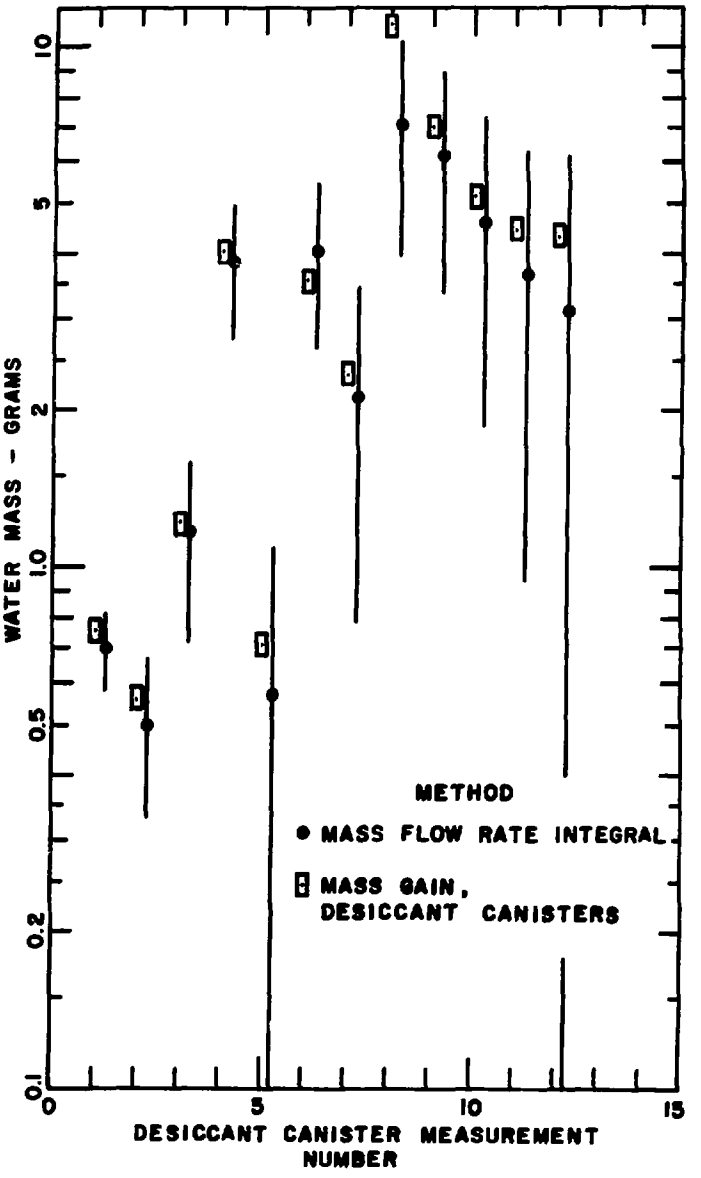

Figure 4. COMPARISON OF TWO WATER MASS LOSS METHODS FOR SALT BLOCK II EXPERIMENT

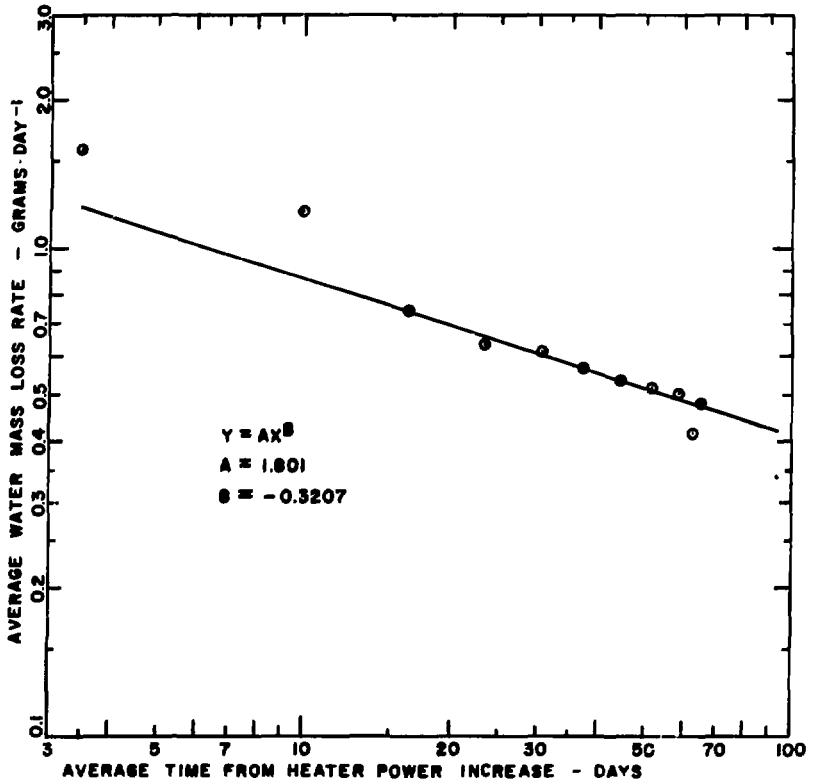

Figure 5. AVERAGE WATER MASS LOSS RATE FOR 1.5 kW HEATING PHASE

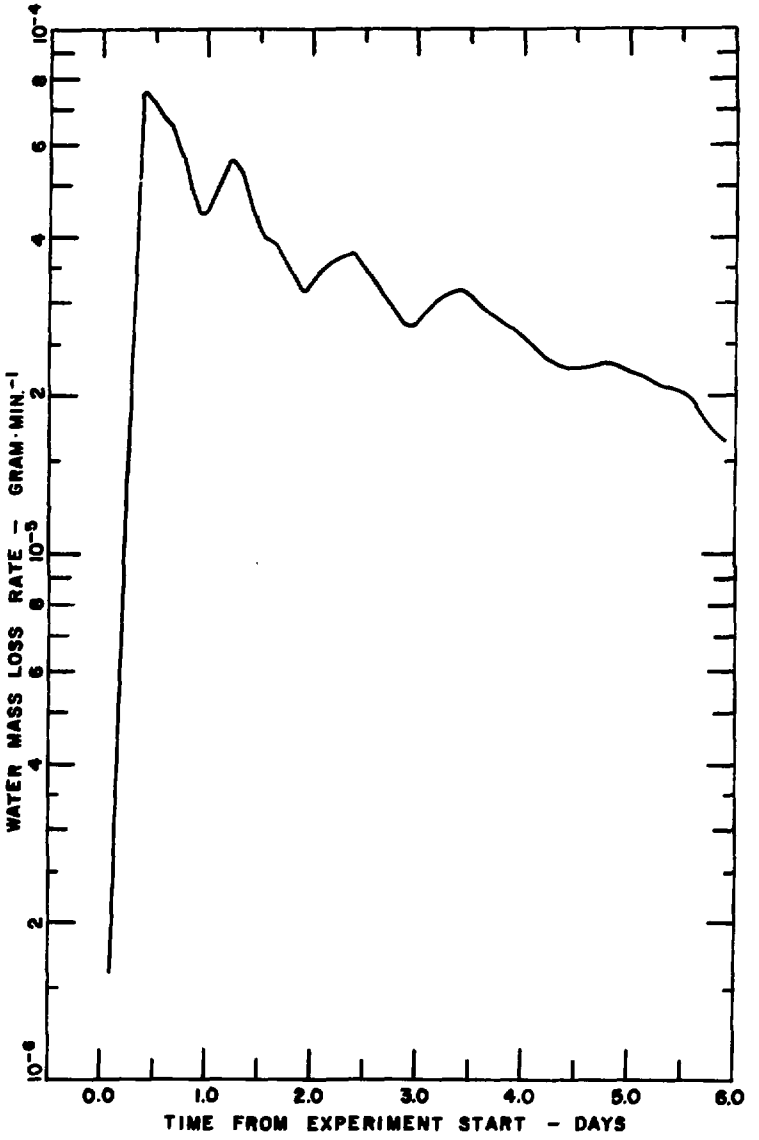

Figure 6. WATER RELEASED AT START OF EXPERIMENT

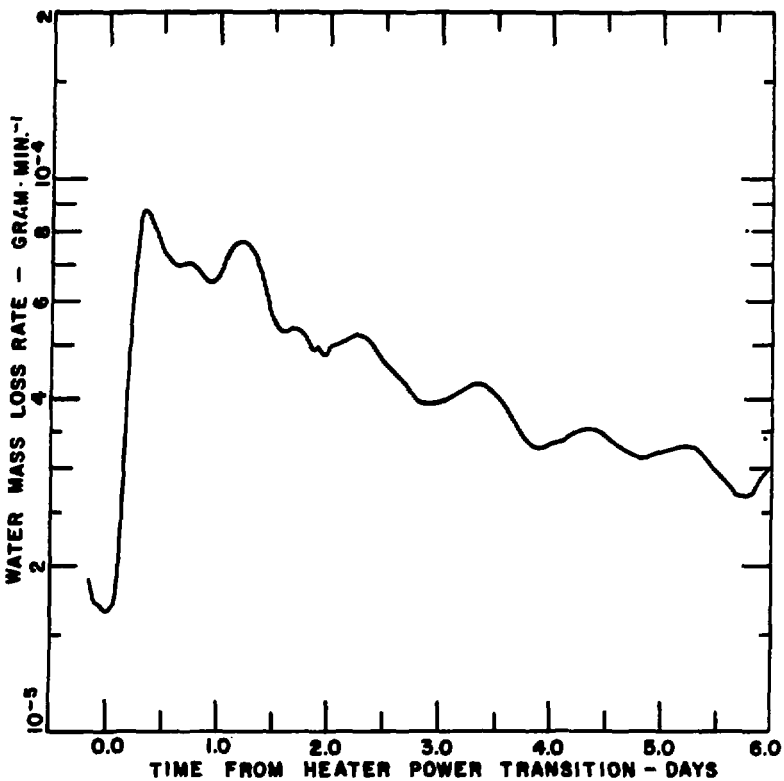

Figure 7. WATER RELEASED AT START OF 0.2 kW HEATER POWER PHASE

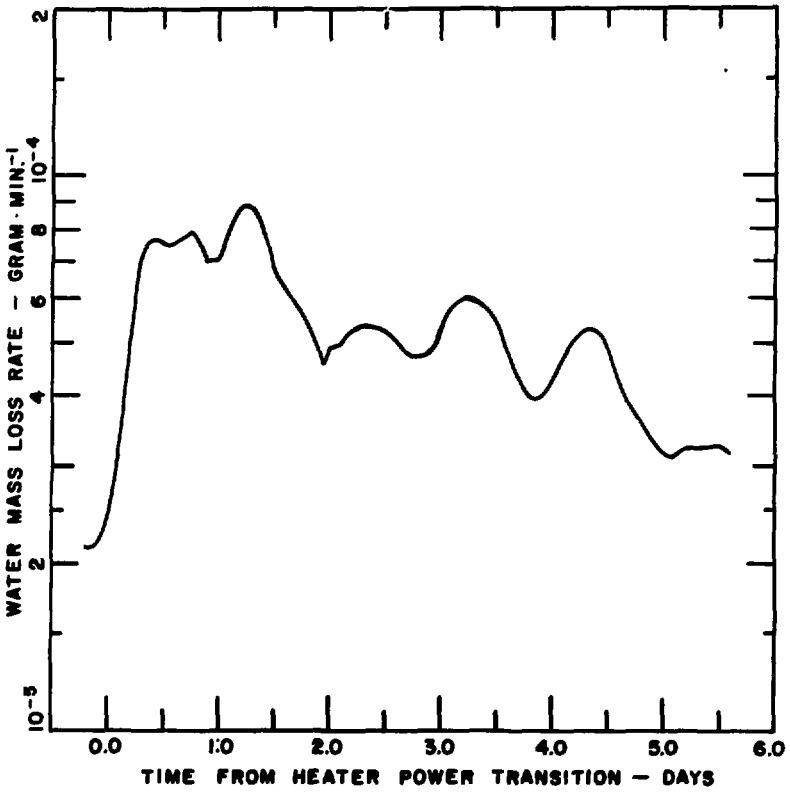

Figure 8. WATER RELEASED AT START OF 0.4 kW HEATER POWER PHASE

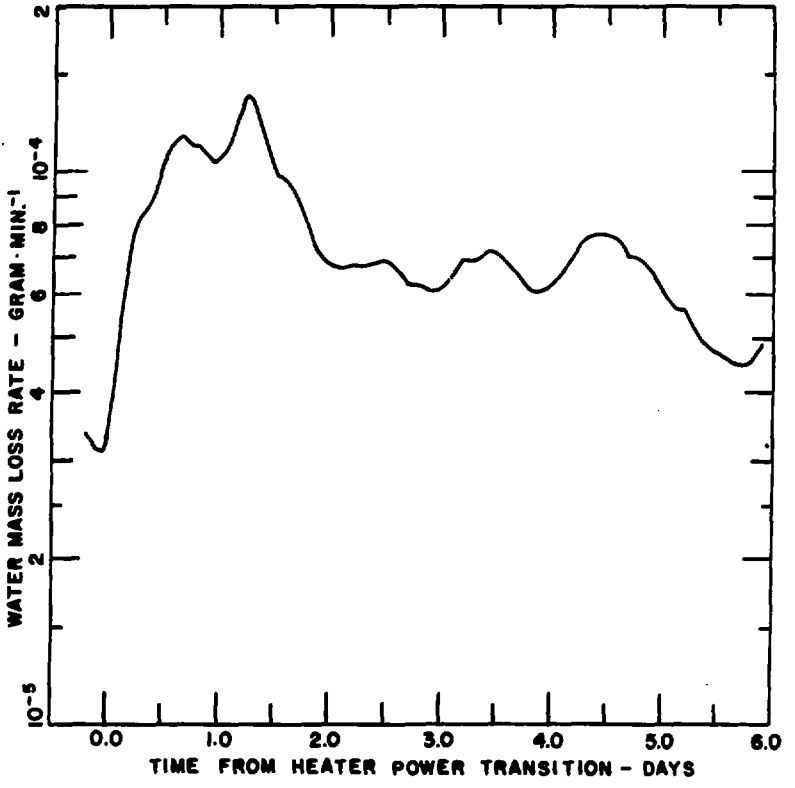

Figure 9. WATER RELEASED AT START OF 0.6 kW HEATER POWER PHASE

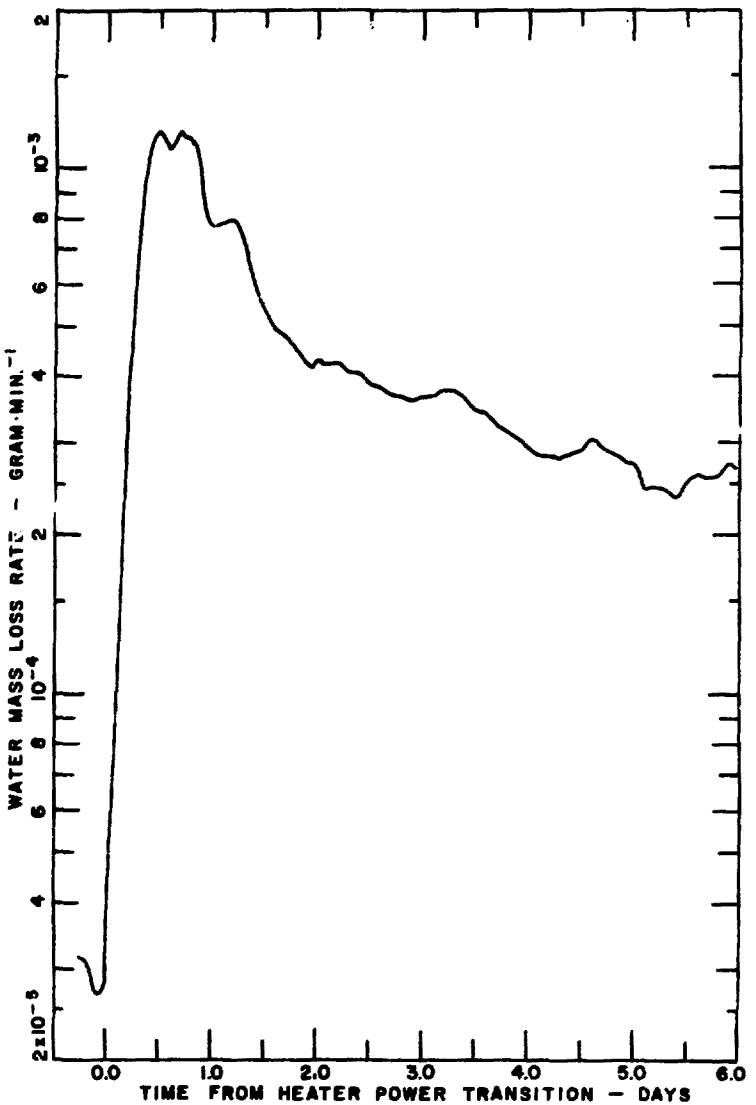

Figure 10. WATER RELEASED AT START OF 1.0 kW HEATER POWER PHASE

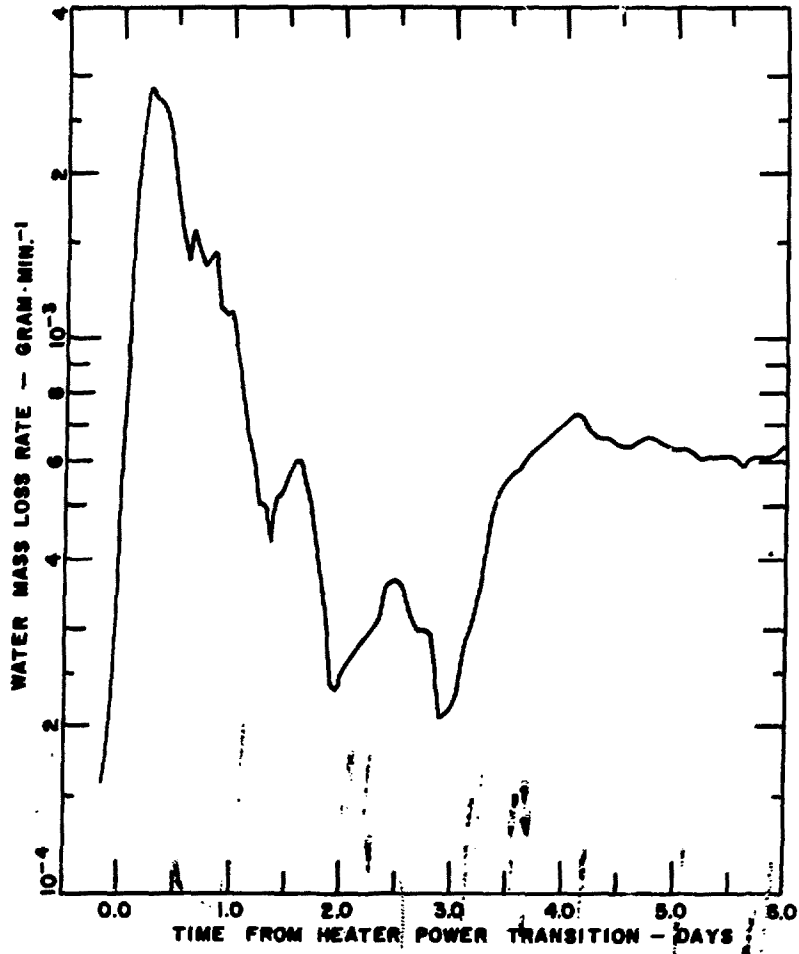

Figure 11. WATER RELEASED AT START OF 1.5 kW HEATER POWER PHASE

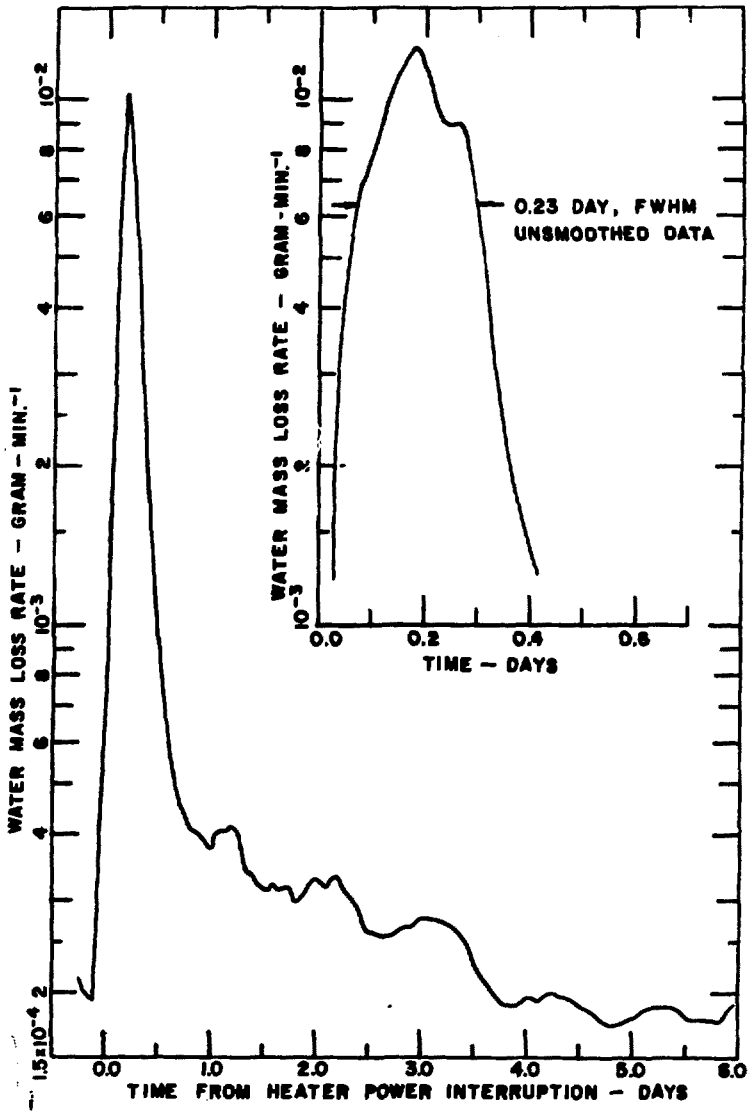

Figure 12. WATER RELEASED AT START OF 1.0 kW HEATER POWER INTERRUPTION PHASE

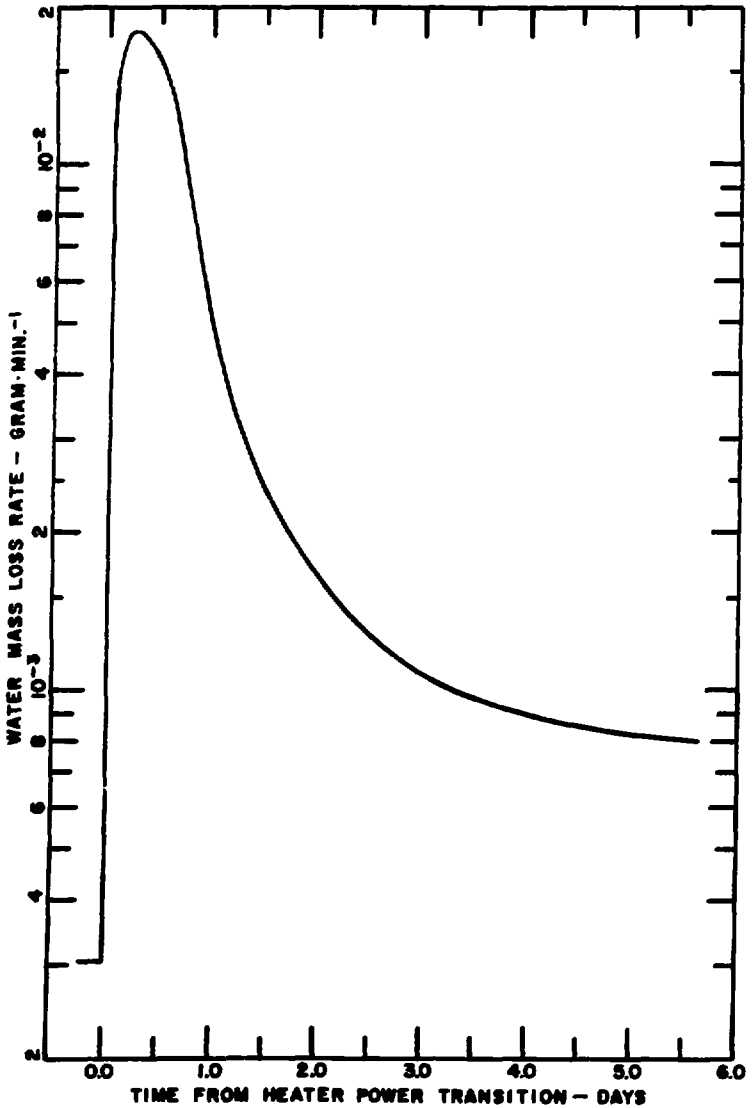

Figure 13. WATER RELEASED AT START OF HEATER POWER SHUTDOWN PHASE, 1.5 kW TO 1.0 kW

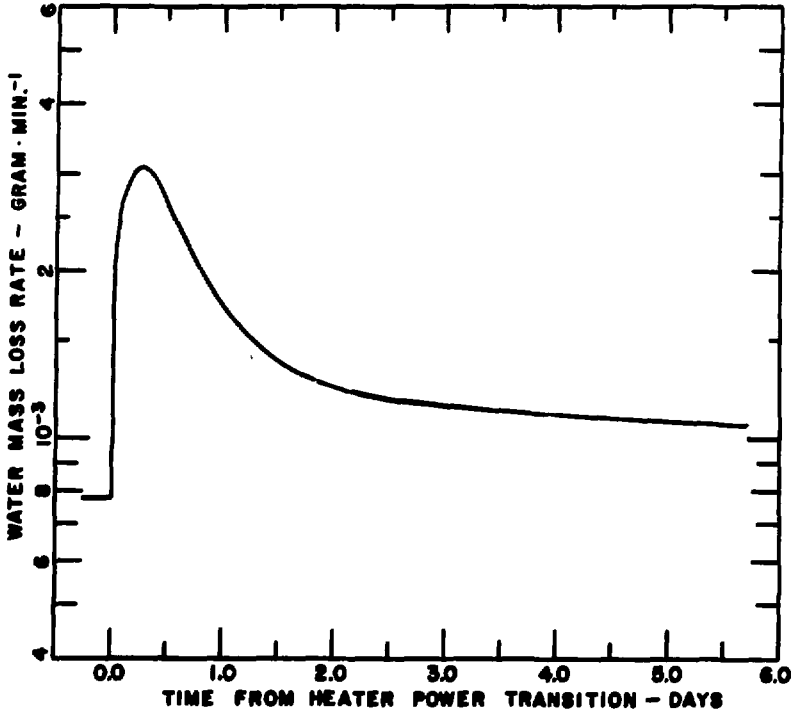

Figure 14. WATER RELEASED AT START OF HEATER POWER SHUTDOWN PHASE, 1.0 kW TO 0.6 kW

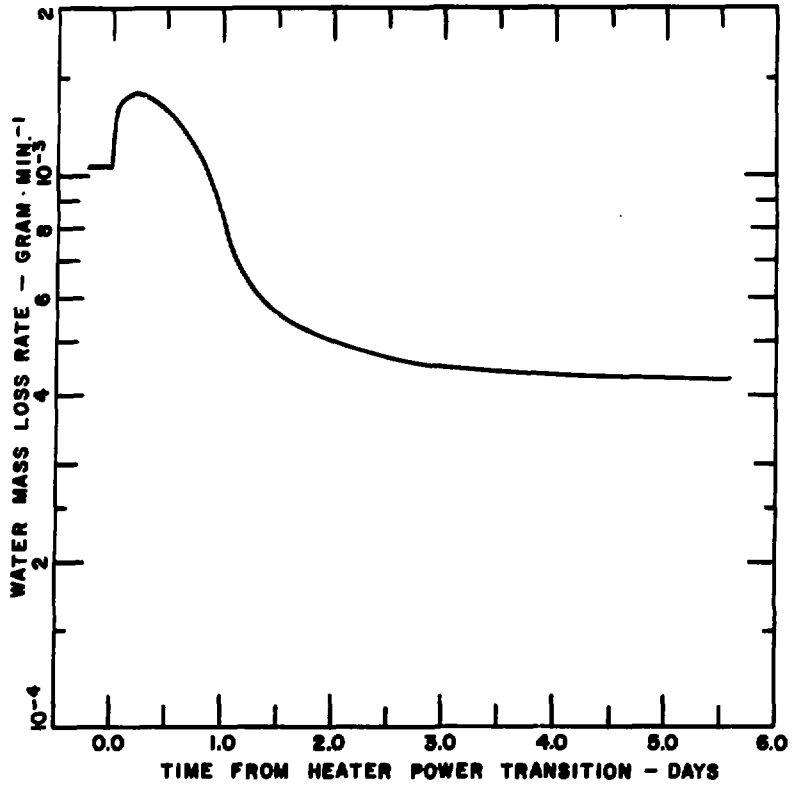

Figure 15. WATER RELEASED AT START OF HEATER POWER SHUTDOWN PHASE, 0.6 kW TO 0 kW

of the five abrupt increases in heater power (Figures 6 through 11) are qualitatively identical. At the beginning of each one of these events, the water mass loss rate increased over a period of about 0.3 day by approximately a factor of ten. The water mass loss rate reached a maximum within 1.0 to 1.5 days after the start of each event, and then it declined slowly and monotonically (except for what appears to be a diurnal effect related to the rise of the salt's enclosure temperature with incident solar radiation). For these six events, the avarage time for the water mass loss rate to decline from its maximum to half its maximum is 1.2 days. The average time for this rate decline is longer (1.8 days) for the three lowest heater power levels than it is for the three highest power levels (0.66 days).

Qualitatively, the water mass loss rate following a decrease in heater power is different from the water mass loss rate following an increase in heater power. The best examples of this phenomenon are presented in Figures 12 and 13 which show, respectively, the water mass loss rates following the heater power interruption at 1.0 kW and following the heater power shutdown from 1.5 kW to 1.0 kW. In these events following a decrease in heater power, one observes a sudden increase in the water mass loss rate by about a factor of 50. This is a transient phenomenon and is followed by an abrupt decline in the water mass loss rate. The water mass loss rate "pulse" shown in Figure 12 has a full width at half maximum of 0.23 days. Figure 13 shows a somewhat wider pulse, but these data are lengthened in time because they were determined at time average rates using the desiccant canister measurements.

Water mass loss as a function of time for the duration of the experiment is presented in Figure 16. Data shown here include the continuous dew-point gage results adjusted to agree with the desiccant canister results at those times for which both measurements were available. Figure 17 shows a "smoothed" water mass loss rate curve for the duration of the experiment. Here the total water mass data (Figure 16) tabulated at 0.5 day intervals was differentiated numerically to provide these rates; consequently peak "average" rates in this figure are less than the peak rates shown in Figures 6 through 15.

Prior to the assembly of the Salt Block II experiment, samples were removed from the salt cylinder's upper surface and analyzed for their water content by measuring their mass loss upon heating to 250°C. Following the

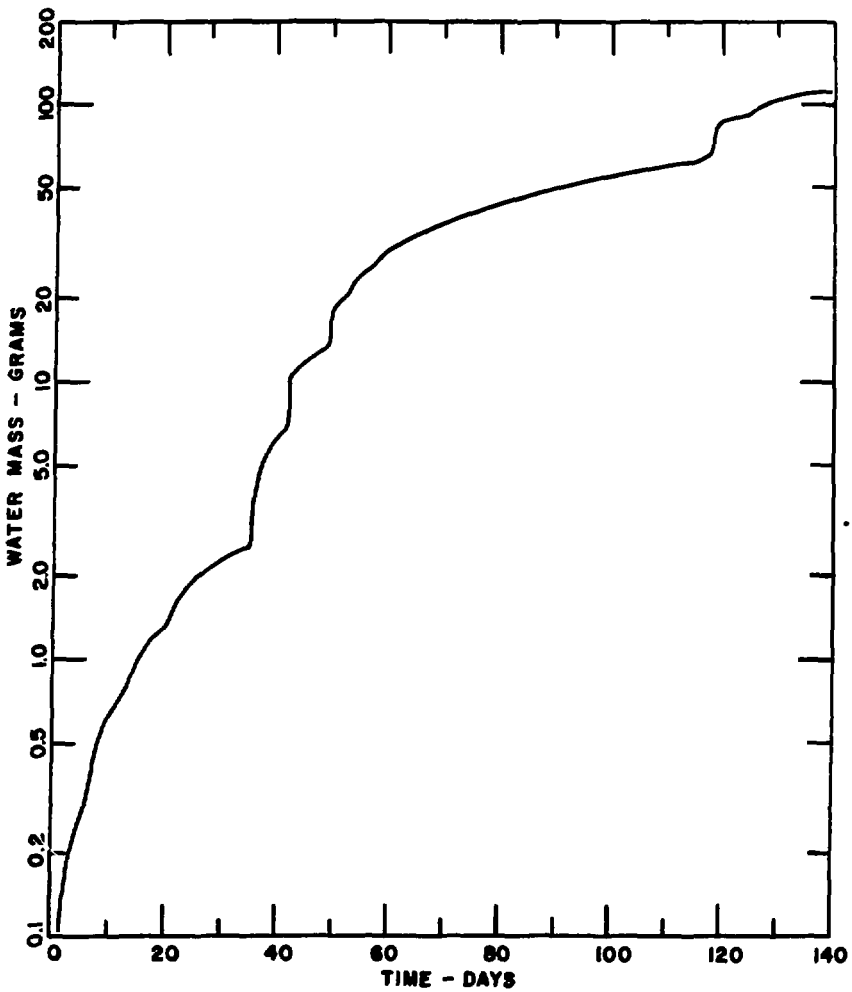

Figure 16. WATER RELEASED IN HEATED BOREHOLE REGION

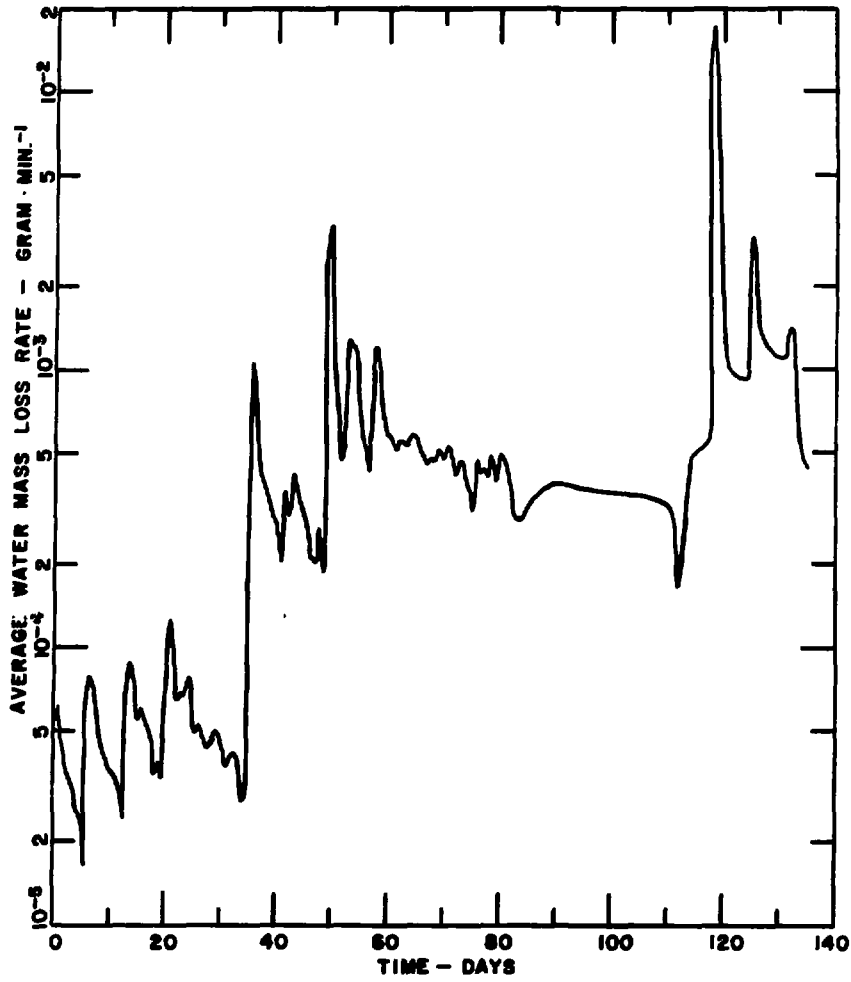

Figure 17. WATER RELEASE RATE IN HEATED BOREHOLE REGION

experiment's disassembly, two sets of samples were taken from the salt block and were analyzed for their water content using the same water-analysis procedure. The purpose of these measurements was to determine the post-experiment spatial distribution of water within the salt block, and if possible, to relate changes in this distribution from the pre-experiment water distribution to the total amount of water released during the course of the experiment. Samples for the first set were taken at different radial positions from the material exposed by cutting and removing a 0.3m-thick slab from the top of the salt block. The process of removing the samples from the test block exposed them to an uncontrolled post-test environment for approximately 40 days prior to their analysis for water content. The samples showed unexpectedly large mass losses upon heating (0.55 $\pm$ 0.17 standard error, mass percent). The second set of samples came from cores which were cut from the salt block following the removal of the 0.3m-thick slab. Specimens from these cores were analyzed within two days following the cores' removal from the block. Specimens from the second set exhibited approximately one-fourth as much mass loss upon heating (0.143 $\pm$ 0.011 standard error, average mass percent) as did the specimens from the first set. Specimens from the first set lost more mass, on the average, than did the pre-test specimens (0.125 $\pm$ 0.020 standard error, average mass percent); however, the average mass loss from the second set of samples agrees, within the limits of error, with the average mass loss from the pre-test samples. The discrepancy between the measurements from the two post-test sets suggests that the post-test environment may have altered the water content of the salt samples. The averages of the results for specimens from both sets of post-test samples are shown in Figure 18. It has not been established whether, as shown here, the apparently relatively lower average water content of the samples taken from salt closest to the experiment's heater was caused by water loss from the salt block during the experiment.

THERMAL BEHAVIOR

The second principal experimental objective was to understand the time-dependent thermal behavior of the Salt Block II experiment.

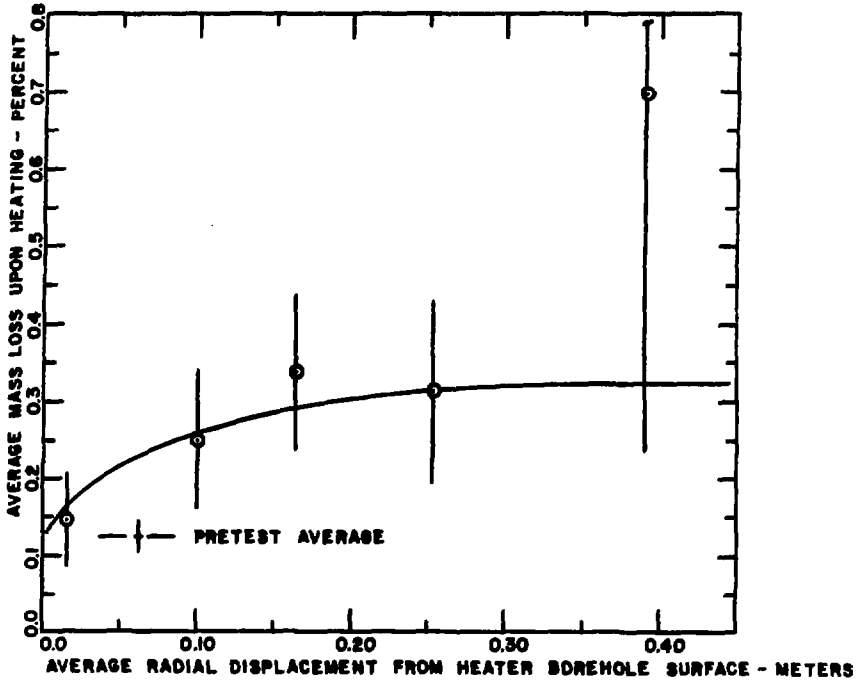

Figure 18. AVERAGE MASS LOSS, UPON HEATING, FOR POSTTEST SAMPLES FROM SALT BLOCK II

In order to determine temperatures and heat fluxes throughout the salt block for the duration of the experiment, 9 heat flux gages and 39 thermocouples were placed at selected locations within and on the block's cylindrical heater, the salt block, and the salt block's containment vessel, and in the environment surrounding the experiment. The experimental geometry was chosen to provide well-defined thermal boundary conditions, for these are necessary if one is to perform any accurate thermal modeling. Figure 19 shows a sectioned, scaled drawing of the assembled experiment and includes thermal sensor locations and relevant dimensions and materials.

Detailed time-dependent thermal calculations were performed by Oscar George (5511), and the final results of these calculations are now available.[2] These calculations were performed using approximate times for heater power changes and nominal values for the heater power. A significant result of the experiment is the power-dependent, non-uniform axial distribution of heater power; a measured, self-consistent set of heater power profiles was used as an input to the thermal modeling calculations.

The power dependent axial variation of temperature within the electric heater was a consequence of its lack of internal baffling as well as its operation at very low power levels. At low electrical power the principal thermal transport mechanism from the heater rods to the heater wall was convection. Consequently only the upper portion of the heater case was effectively heated. For heater powers in excess of 1.0 kW radiant transport from the heater elements to the heater case was dominant, and the heater's resultant temperature profile was more nearly symmetric about its midplane.

Results of the calculations include best fit values for the thermal conductivity of the salt and crushed salt backfill as well as predicted values of temperature and heat flux (where appropriate) at each thermal sensor location. Independent calculations of the salt's thermal conductivity were performed using the measured temperatures and heat fluxes along the midplane of the salt block. The two sets of thermal conductivity versus temperature data are presented in Figure 20.

In general, at the location of each thermal sensor, agreement between predicted and measured temperatures is within several degrees Celsius, but only a selected small fraction of all the measured and predicted thermal

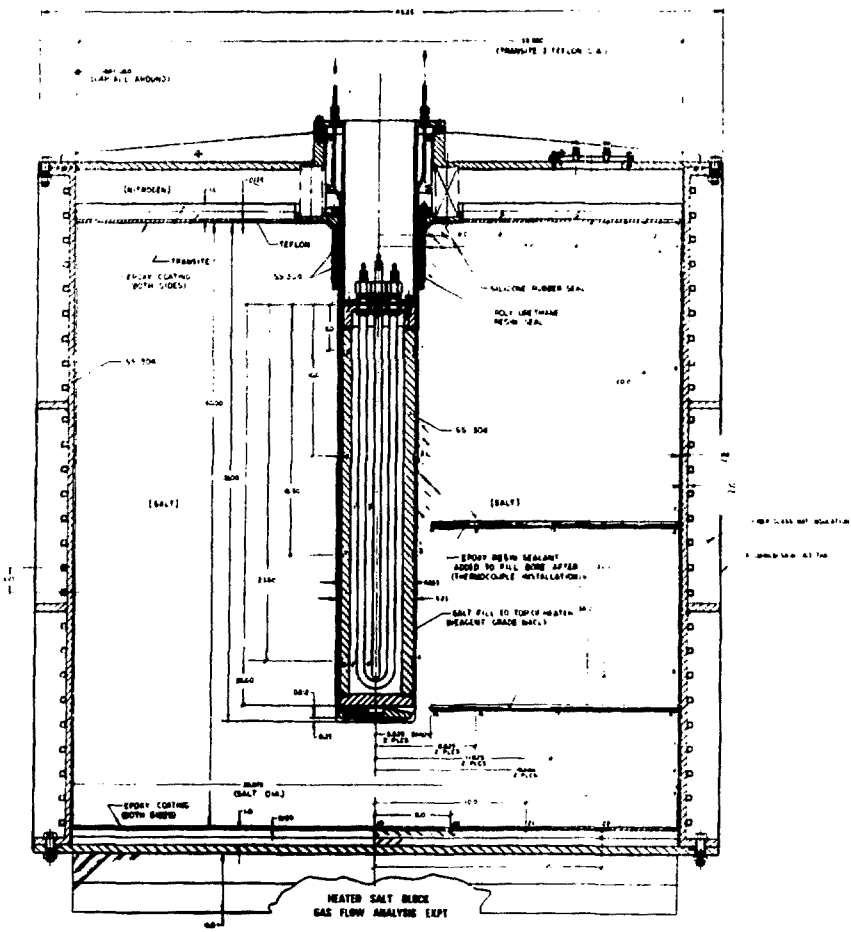

Figure 19. SALT BLOCK II EXPERIMENT ASSEMBLY

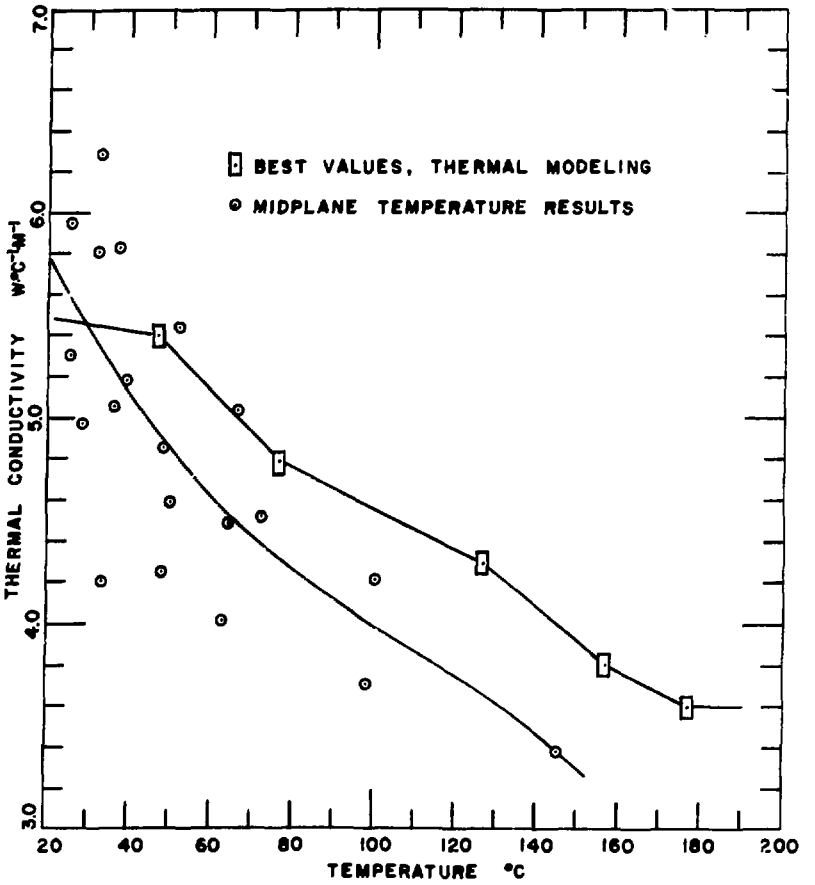

Figure 20. THERMAL CONDUCTIVITY OF GEOLOGIC SALT USED IN SALT BLOCK II EXPERIMENT

data is presented here. Figures 21, 22, 23, and 24 show the measured and predicted temperatures for the four thermocouples located in the mid-plane of the salt block for the period following the heater power transition from 0.2 to 0.4 kW. One result of note here is that the e-folding time* for temperature is position dependent, although throughout most of the salt block, the e-folding times are approximately 0.5 days. Measured and theoretical equilibrium temperatures as well as e-folding times for the 0.4 kW heater power level are presented in Table III. Temperatures measured by the 4 thermocouples located along the midplane of the salt block (borehole A) for the duration of the experiment are shown in Figures 25 through 28.

The calculated equilibrium temperature distribution within the salt block is shown in a scaled illustration for each of the 5 heater power levels in Figures 29 through 33. The temperature shown in each box represents the temperature at the geometric midpoint of that volume within the salt block. From these data, numerical methods can be used to calculate the equilibrium values of both temperature and temperature gradient at any point within the salt block. The data shown in Figures 29 through 33 were differentiated numerically to obtain the radial component of the thermal gradient evaluated at the midpoint of each "cell" used in the thermal analysis. The absolute values of these data (all radial components were negative) are shown for the 5 heater power levels in Figures 34 through 38.

DATA ANALYSIS

Data from selected channels from the H.P. 3052A data acquisition system have been printed to enable a preliminary comparison of the thermal predictions with the measured temperatures. The analysis of the measured water-loss rate is essentially complete, and these data have been presented here. The experimental data recorded on approximately 50 Hewlett-Packard floppy

* The e-folding time is the time it takes for temperature changes at a given location to come within e^{-1} of the temperature difference between the equilibrium temperatures before and after the time of thermal change.

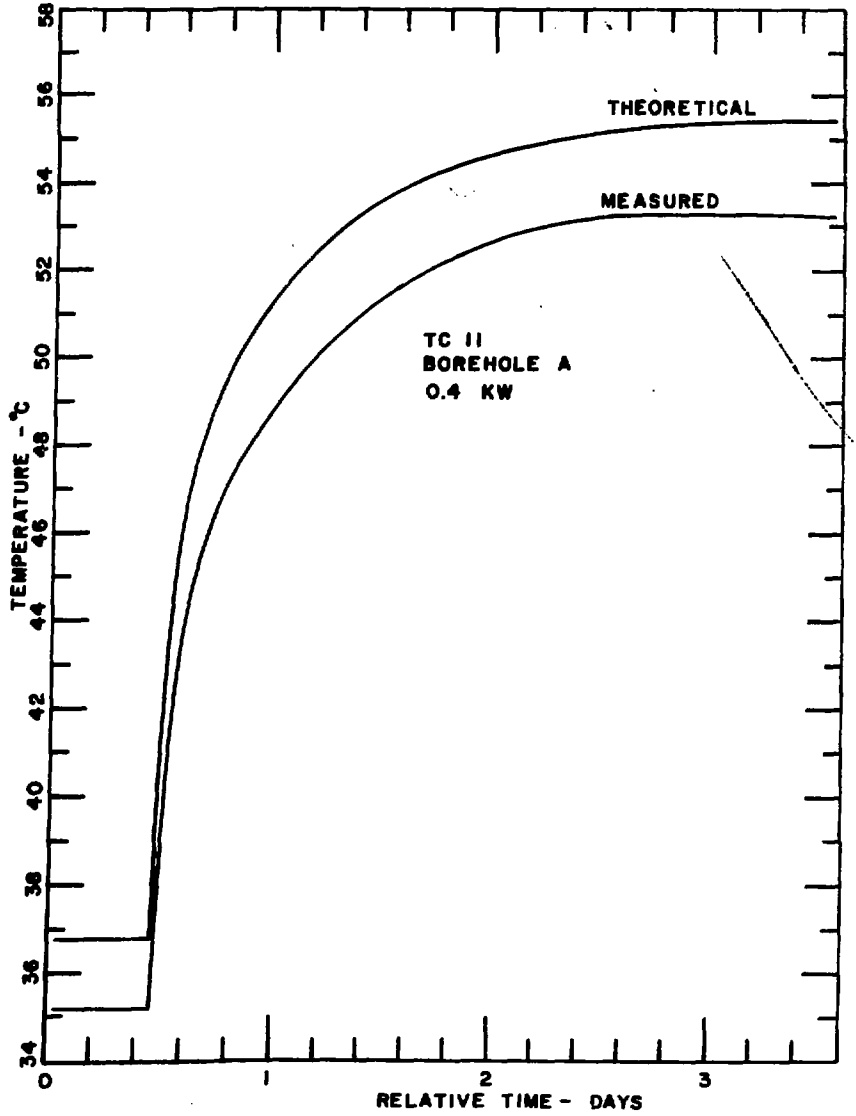

Figure 21. TEMPERATURE OF THERMOCOUPLE 11 FOR THE HEATER POWER TRANSITION FROM 0.2 kW TO 0.4 kW

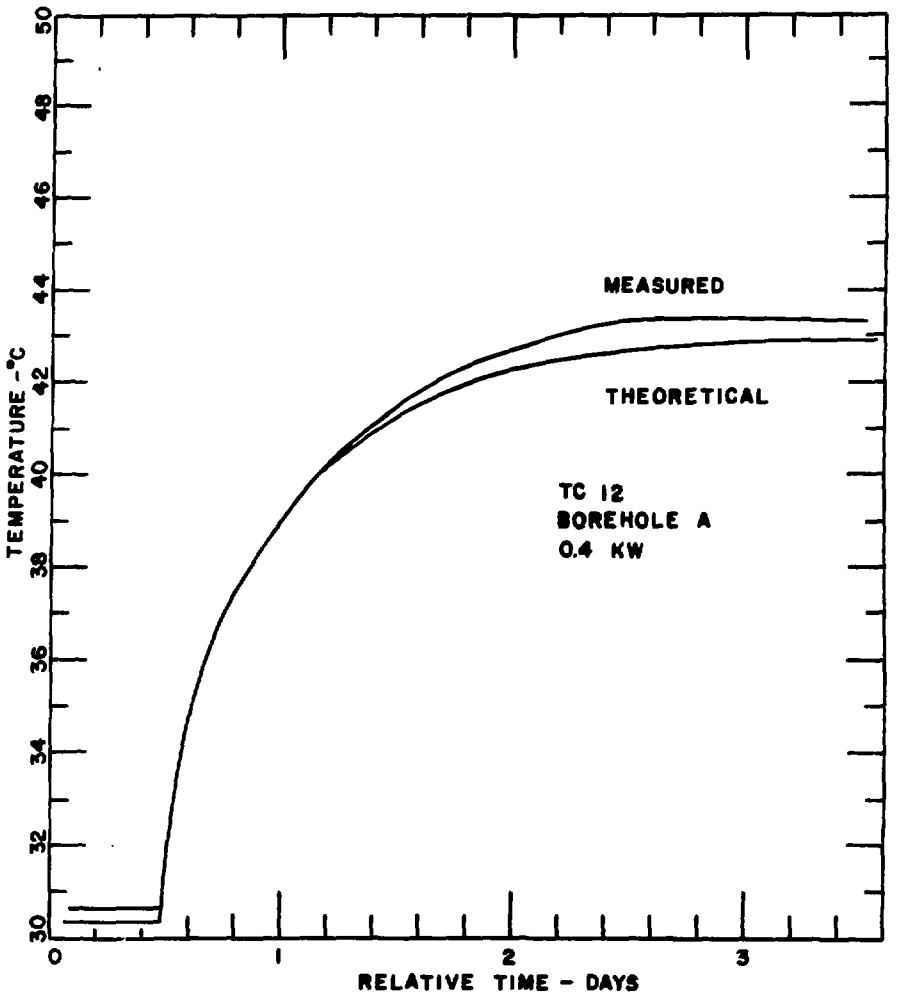

Figure 22. TEMPERATURE OF THERMOCOUPLE 12 FOR THE HEATER POWER TRANSITION FROM 0.2 kW TO 0.4 kW

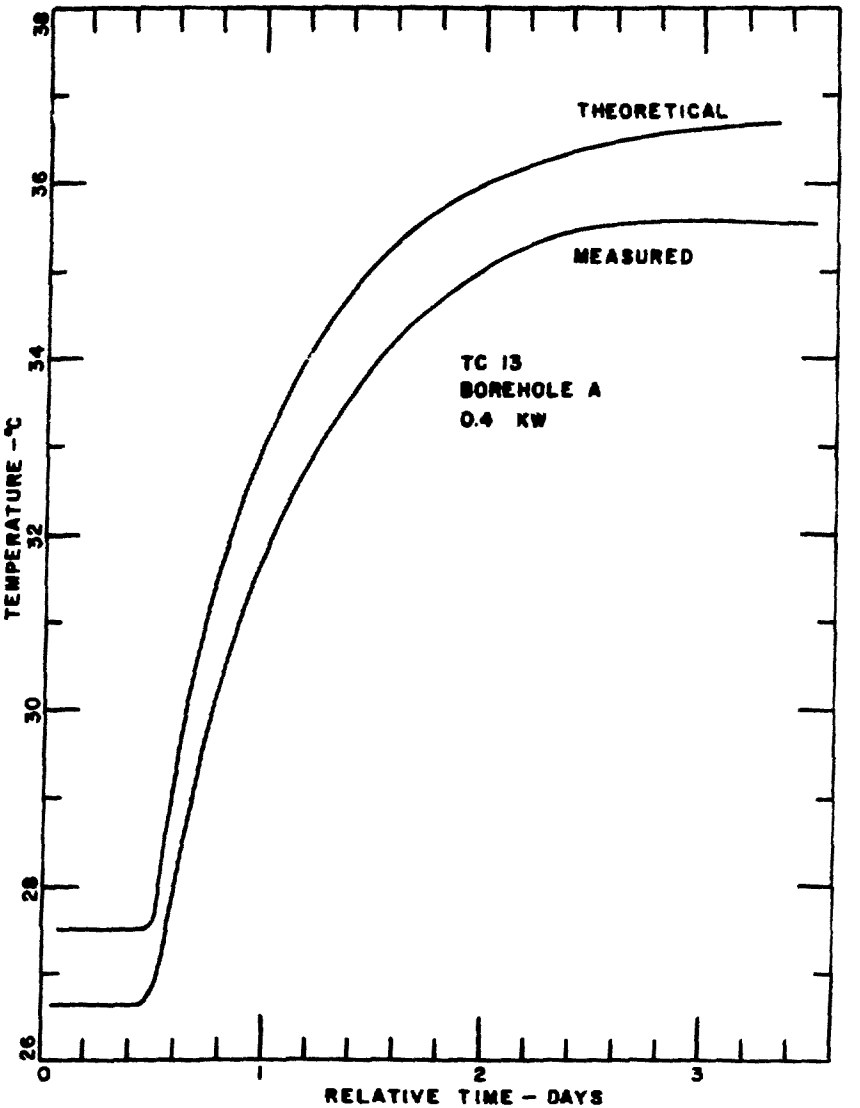

Figure 23. TEMPERATURE OF THERMOCOUPLE 13 FOR THE HEATER POWER TRANSITION FROM 0.2 kW TO 0.4 kW

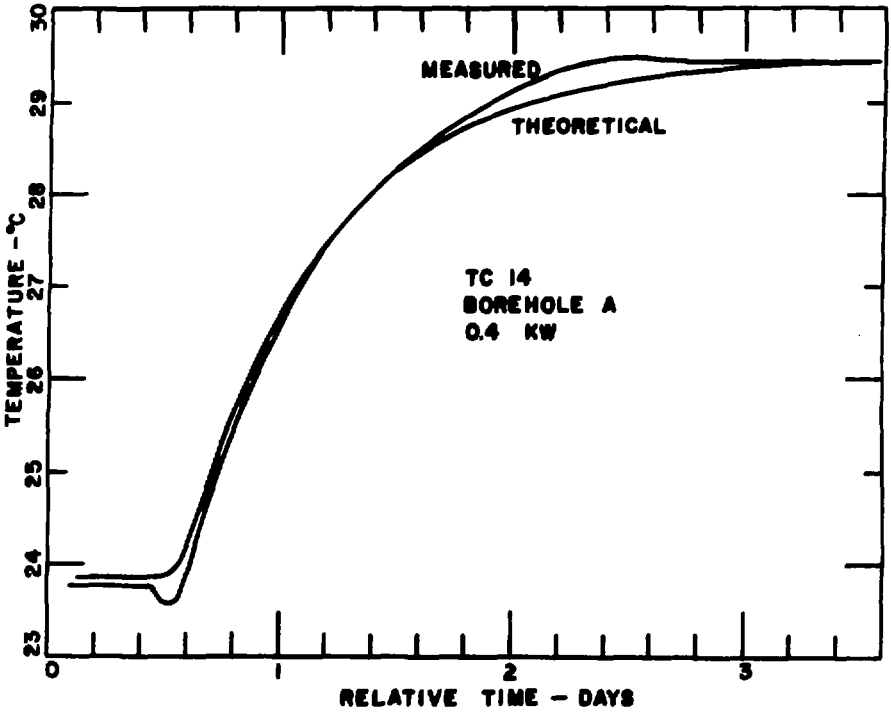

Figure 24. TEMPERATURE OF THERMOCOUPLE 14 FOR THE HEATER POWER TRANSITION FROM 0.2 kW TO 0.4 kW

TABLE III

Salt Block II Temperatures, Transition From 0.2 kW to 0.4 kW

Thermocouple Number	Theoretical				Measured			
	Initial Temperature °C	Final Temperature °C	Temperature Change °C	e-Folding Time Days	Initial Temperature °C	Final Temperature °C	Temperature Change °C	e-Folding Time Days
5	52.41±.004	81.90±.09	29.49±.09	0.32	51.87±.07	83.78±.14	31.91±.16	0.27
6	50.33±.004	79.49±.09	29.16±.09	0.33	49.00±.09	80.80±.15	31.80±.17	0.30
7	45.40±.004	73.65±.09	28.25±.09	0.33	44.85±.07	73.19±.15	28.34±.17	0.32
8	32.69±.004	52.74±.09	20.05±.08	0.40	35.33±.07	54.52±.15	19.19±.17	0.41
9	27.05±.003	34.56±.07	7.51±.07	0.66	27.66±.04	35.98±.08	8.32±.09	0.52
10	25.17±.003	31.13±.06	5.96±.06	0.69	25.62±.03	32.00±.07	6.38±.08	0.55
11	36.79±.004	55.55±.08	18.76±.08	0.43	35.17±.23	53.14±.12	17.97±.26	0.45
12	30.63±.004	43.01±.07	12.38±.07	0.53	30.36±.08	43.22±.12	12.86±.14	0.52
13	27.51±.004	36.74±.07	9.23±.07	0.60	26.67±.05	35.52±.11	8.85±.12	0.59
14	23.87±.002	29.47±.05	5.60±.05	0.66	23.76±.05	29.42±.14	5.66±.15	0.62
15	27.44±.003	38.83±.07	11.39±.07	0.55	28.08±.07	39.30±.09	11.22±.11	0.56
16	25.76±.003	34.53±.07	8.77±.07	0.62	26.22±.06	35.11±.08	8.89±.10	0.62
17	24.53±.003	31.63±.06	7.10±.06	0.66	24.39±.06	31.17±.09	6.78±.11	0.67
18	22.46±.002	27.12±.05	4.66±.05	0.71	22.38±.04	27.11±.10	4.73±.11	0.70
19	24.12±.003	31.17±.06	7.05±.06	0.66	23.83±.03	30.00±.04	6.17±.05	0.74
20	23.82±.003	30.45±.06	6.63±.06	0.67	23.51±.09	29.33±.05	5.82±.10	0.77
21	23.16±.003	28.88±.06	5.72±.06	0.70	*23.03±.62	*27.41±1.36	--	--
22	22.37±.002	27.09±.05	4.72±.05	0.73	21.84±.07	26.06±.02	4.22±.07	0.76

*Defective sensor cold junction.

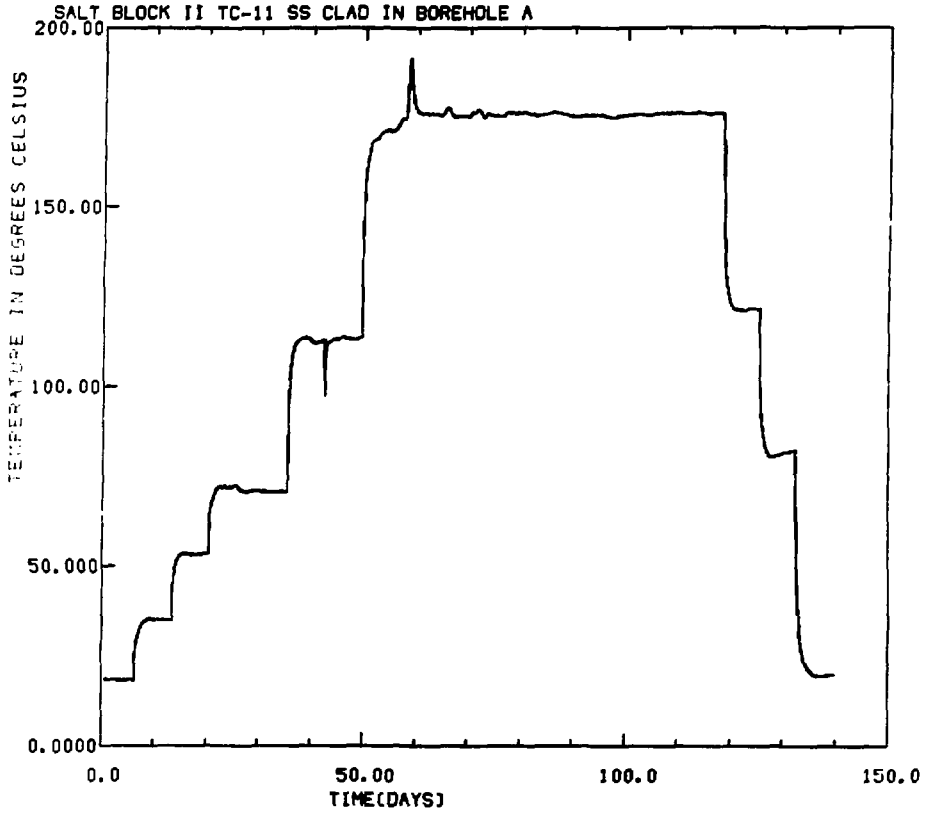

Figure 25. TEMPERATURE MEASURED BY THERMOCOUPLE 11 IN MIDPLANE OF SALT BLOCK

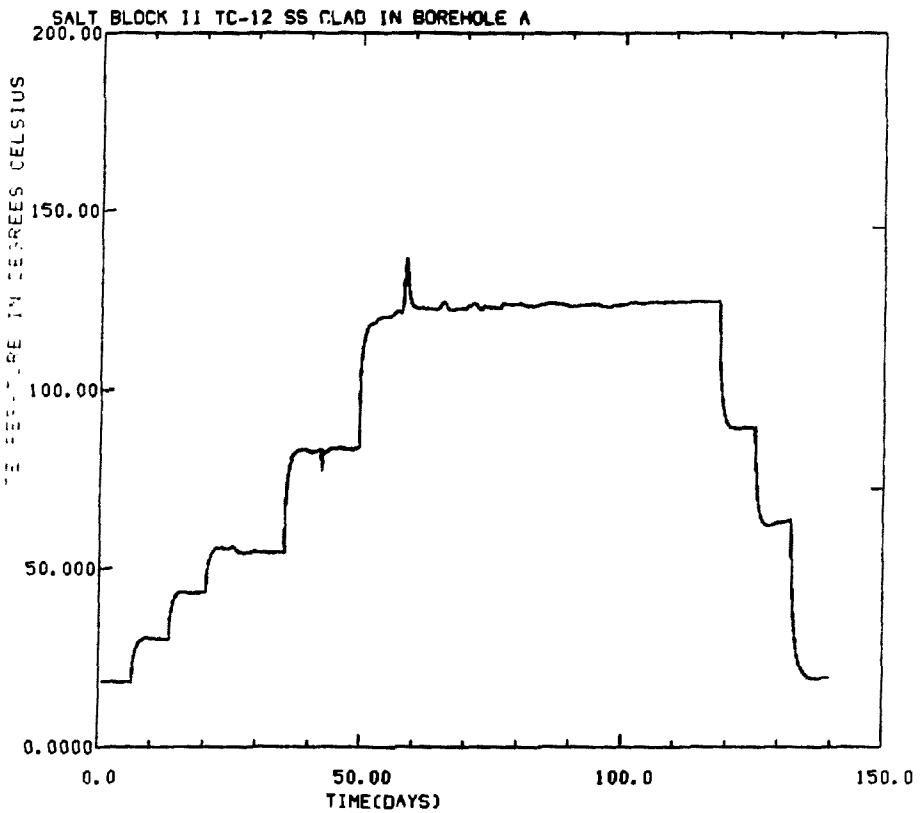

Figure 26. TEMPERATURE MEASURED BY THERMOCOUPLE 12 IN MIDPLANE OF SALT BLOCK

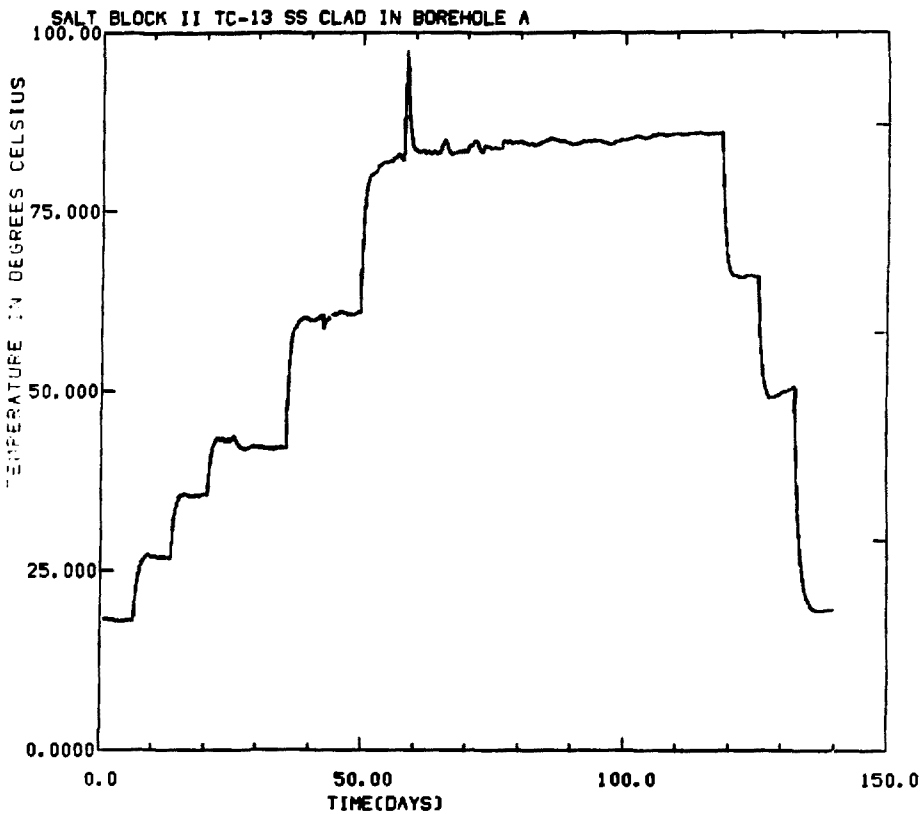

Figure 27. TEMPERATURE MEASURED BY THERMOCOUPLE 13 IN MIDPLANE OF SALT BLOCK

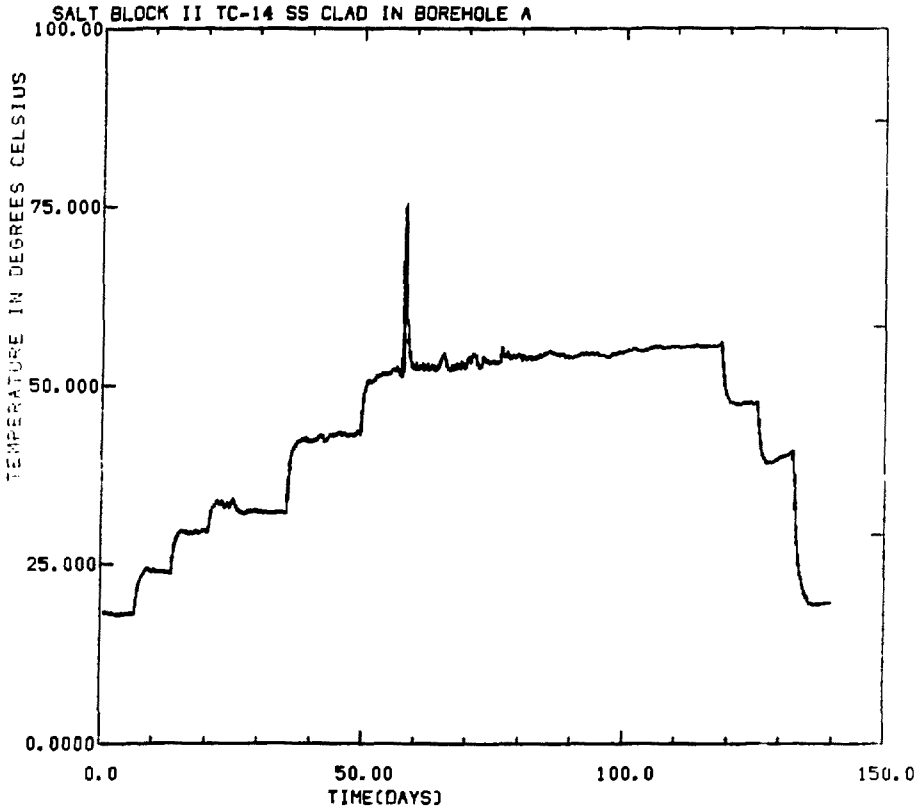

Figure 23. TEMPERATURE MEASURED BY THERMOCOUPLE 14 IN MIDPLANE OF SALT BLOCK

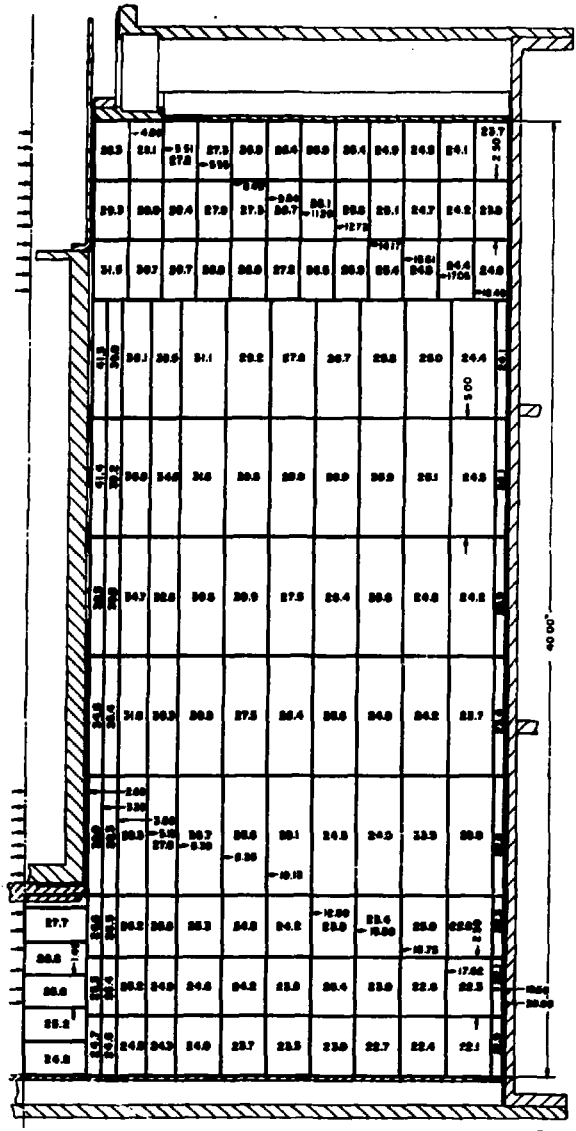

Figure 29. CALCULATED EQUILIBRIUM TEMPERATURES (°C) IN SALT BLOCK FOR 0.2 kW HEATER POWER

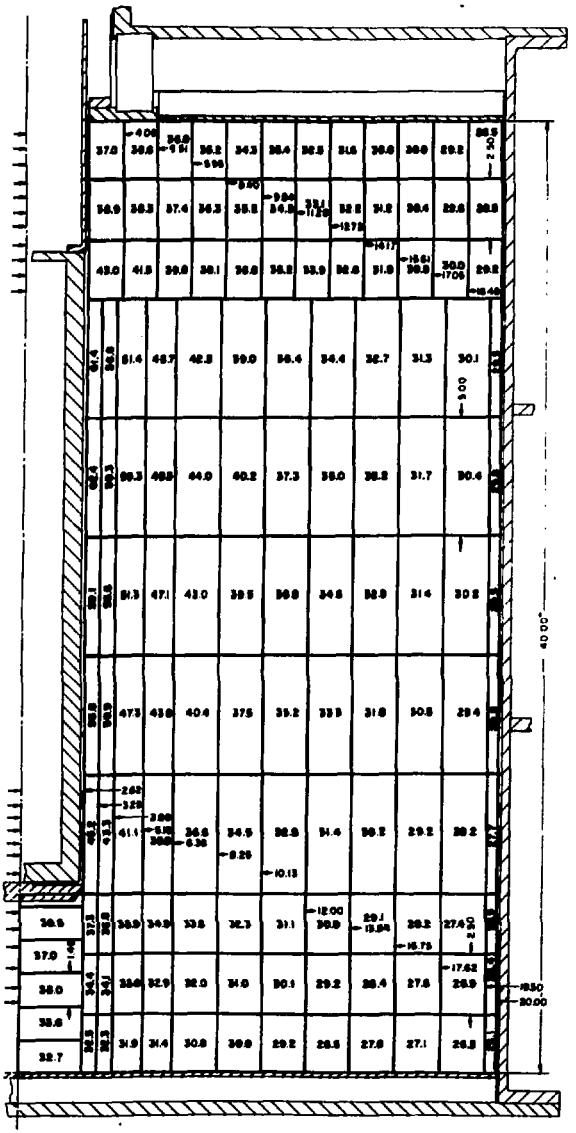

Figure 30. CALCULATED EQUILIBRIUM TEMPERATURES (°C) IN SALT BLOCK FOR 0.4 kW HEATER POWER

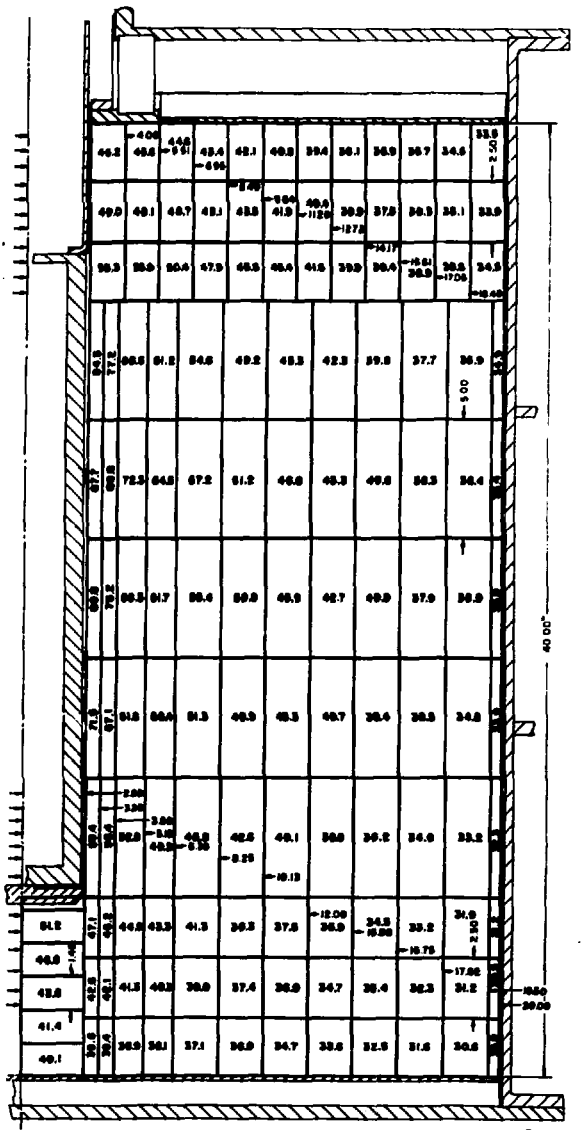

Figure 31. CALCULATED EQUILIBRIUM TEMPERATURES (°C) IN SALT BLOCK FOR 0.6 kW HEATER POWER

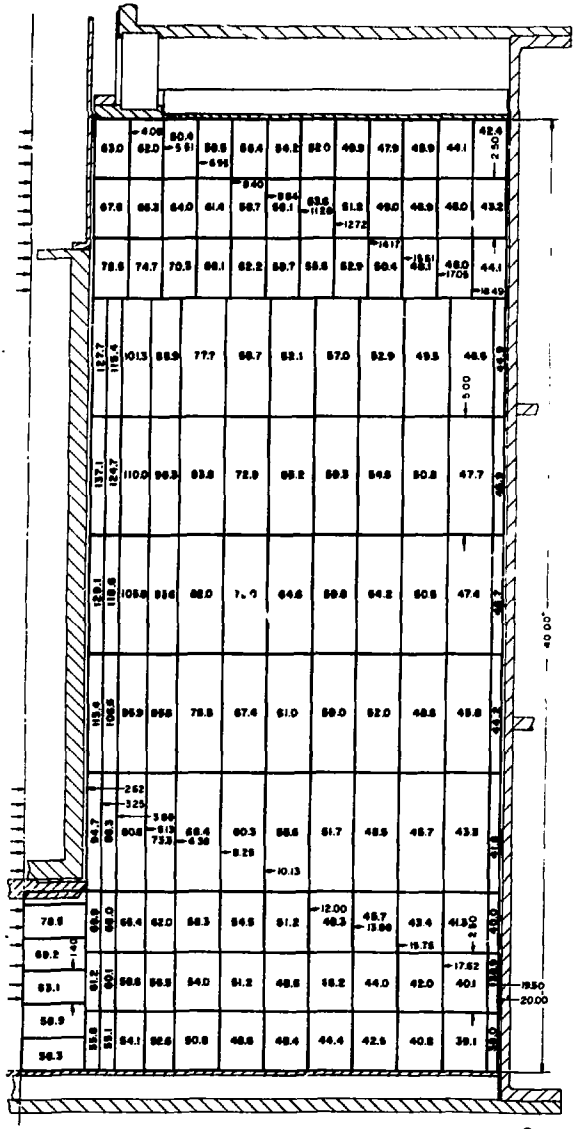

Figure 32. CALCULATED EQUILIBRIUM TEMPERATURES (^{o}C) IN SALT BLOCK FOR 1.0 kW HEATER POWER

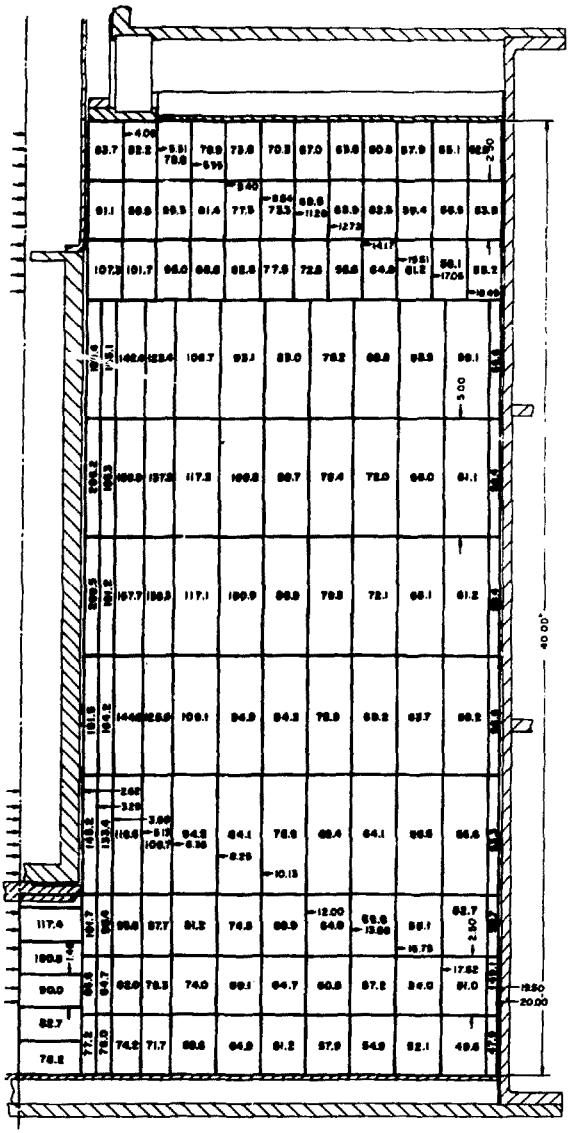

Figure 33. CALCULATED EQUILIBRIUM TEMPERATURES (^{o}C) IN SALT BLOCK FOR 1.5 kW HEATER POWER

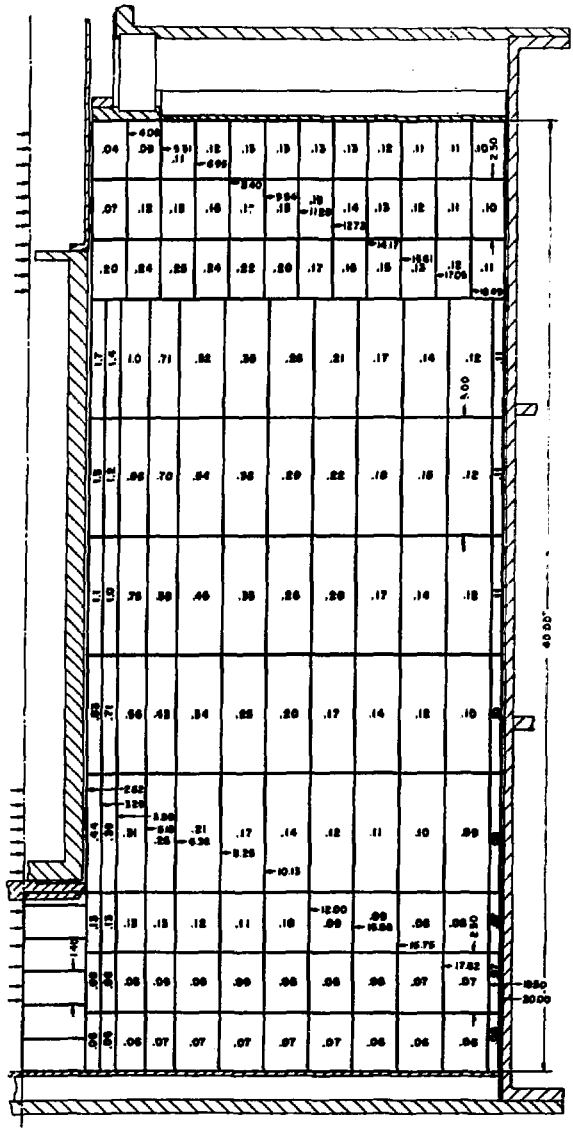

Figure 34. ABSOLUTE VALUE OF THE CALCULATED RADIAL COMPONENT OF THE EQUILIBRIUM THERMAL GRADIENT ($^{o}C \cdot cm^{-1}$) IN SALT BLOCK FOR 0.2 kW HEATER POWER

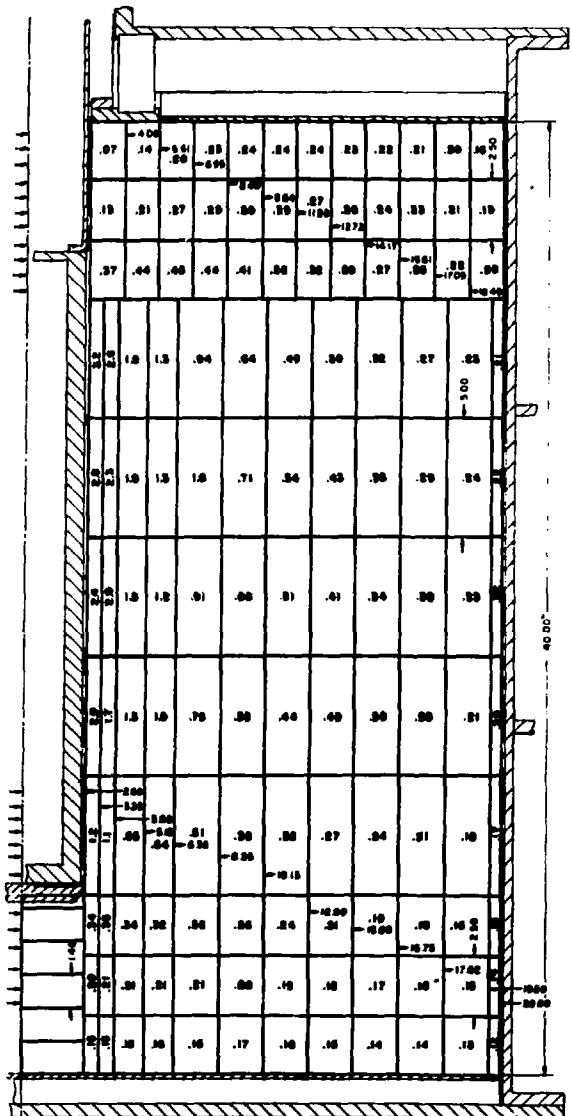

Figure 35. ABSOLUTE VALUE OF THE CALCULATED RADIAL COMPONENT OF THE EQUILIBRIUM THERMAL GRADIENT ($^{o}C \cdot cm^{-1}$) IN SALT BLOCK FOR 0.4 kW HEATER POWER

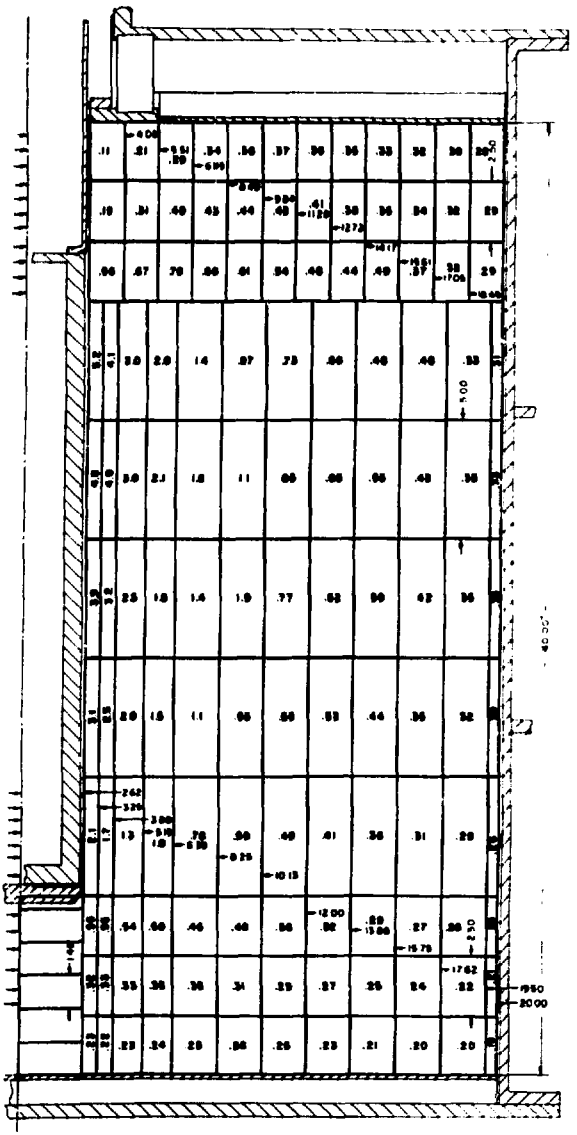

Figure 36. ABSOLUTE VALUE OF THE CALCULATED RADIAL COMPONENT OF THE EQUILIBRIUM THERMAL GRADIENT ($^{o}C \cdot cm^{-1}$) IN SALT BLOCK FOR 0.6 kW HEATER POWER

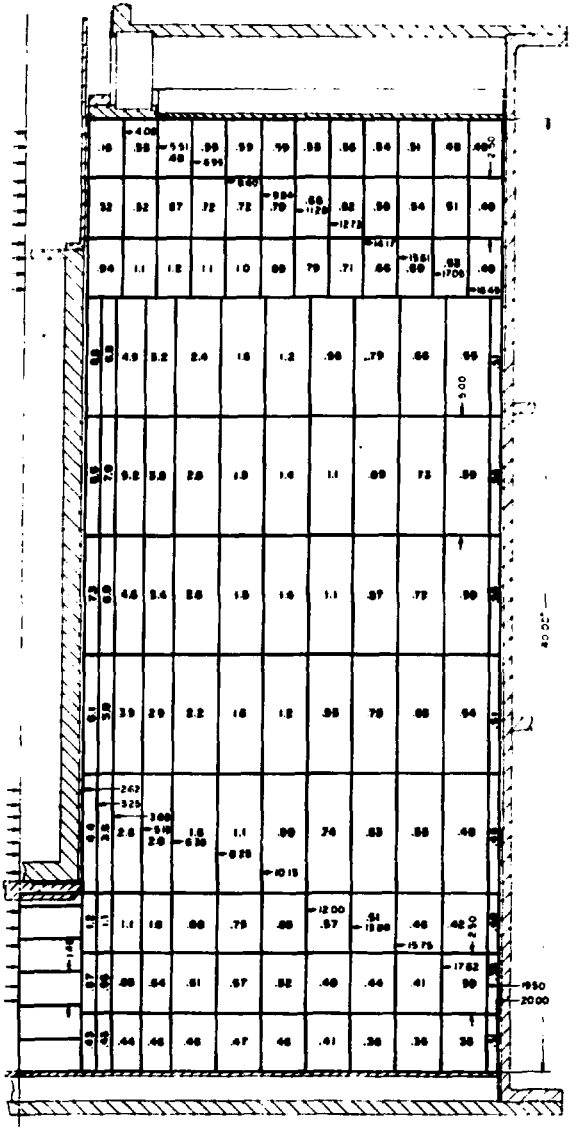

Figure 37. ABSOLUTE VALUE OF THE CALCULATED RADIAL COMPONENT OF THE EQUILIBRIUM THERMAL GRADIENT ($^{o}C \cdot cm^{-1}$) IN SALT BLOCK FOR 1.0 kW HEATER POWER

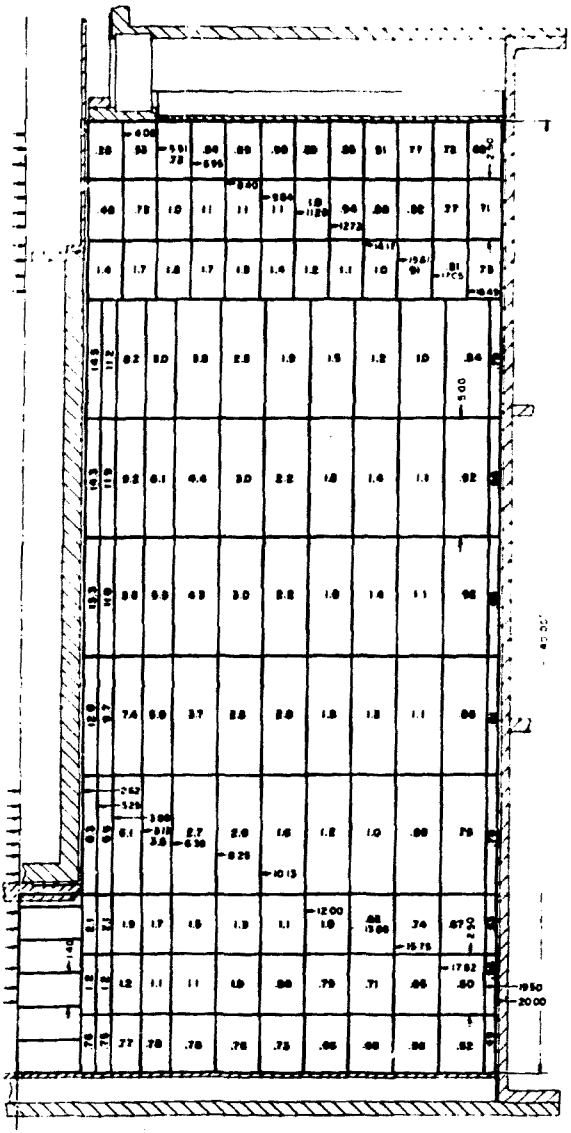

Figure 38. ABSOLUTE VALUE OF THE CALCULATED RADIAL COMPONENT OF THE EQUILIBRIUM THERMAL GRADIENT ($^{o}C \cdot cm^{-1}$) IN SALT BLOCK FOR 1.5 kW HEATER POWER

disks have been copied onto 9-track magnetic tape. These data will be transferred, in part, onto 7-track magnetic tape as permanent files.

DISCUSSION

The most significant observations of this experiment are the time-dependent nature of the water release rates. Large increases in the water release rate are observed following changes in the heater power. The greatest water-release rates were observed following decreases in the heater power. The measured water-release rates are in qualitative agreement with similar measurements made on heated 1 kg salt samples. Ron Hadley (5511) is developing a water transport model that predicts water-release rates that agree quantitatively with the measured water-release rates. It appears that the thermomechanical response of the salt, including the stress state and time-dependent stress relaxation, is an essential ingredient in predicting the measured water release rates.[3] The large increase in the water flow rate following a decrease in the heater power arises because the salt fails in tension with the resultant increase in its permeability.

The total water released during the experiment (111.4 gm) is small compared to the block's water content (from between 2.2 kg and 9.0 kg). The data presented in Figure 18 provide some indication of water depletion in the material surrounding the borehole at distances up to about 0.08 m from the borehole's surface. Note that the water content of this annular volume surrounding the borehole lies between 32 g and 133 g which is of the order of that which was released into the borehole. Significant water transport probably occurred only in a small region surrounding the borehole.

Microscopic examination of the post-test cored salt from material adjacent to the borehole revealed radially oriented tracks, which were highly non-uniform in length (up to 10 mm long) and spatial distribution. Some of these tracks contained fluid.[4] Similar tracks were not observed in comparable but unheated geologic salt. These tracks may be evidence of the physical transport of fluids along thermal gradients, but their significance to the evolved water measured in this experiment has not been established.

The good agreement between thermal measurements and calculated values of the thermal field within the salt block indicate that our knowledge of the salt block's time-dependent temperature distribution is adequate for any post-test analyses or modeling. In this regard, the vertical spatial distribution of power from the cylindrical heater was not only non-uniform but varied with heater power. For low heater power levels (up to 0.4 kW), most of the heater's power is released from its upper portion while at high heater power (greater than 1.0 kW), the spatial distribution of the heater's power shifts toward the heater's midplane. Measured values of the salt's thermal conductivity in the region from 18°C to 200°C range from 5.5 $w^{o}c^{-1}$ m^{-1} to 3.6 $w^{o}c^{-1}.m^{-1}$ at these temperatures, respectively; these are consistent with other measurements of thermal conductivity determined on smaller samples.[5]

Further analysis of the data is not expected to alter significantly the material presented here. "Fine-tuning" of the thermal model by introducing, for example, a time-dependent, thermal resistance at the salt-stainless steel shell interface is possible although unnecessary for anticipated water-transport calculations. Post-test chemical analysis of the crushed salt backfill around the heater and chemical and mineralogical analysis of the salt block are continuing. Analyses of the backfill material are consistent with the measured water released into the borehole region. Refinement of existing water-transport models to include the thermomechanical properties of the salt, together with the salt block's time-dependent temperature field, in order to predict water transport rates is where subsequent efforts should be expended.

REFERENCES

1. Hohlfelder, J. J., Measurement of Water Lost From Heated Geologic Salt, SAND79-0462, Sandia National Laboratories, Albuquerque, New Mexico, 1979.

2. George, O., Computer Thermal Modeling for the Salt Block II Experiment, SAND79-2250, Sandia National Laboratories, Albuquerque, New Mexico (to be published).

3. Hohlfelder, J. J. and G. R. Hadley, Laboratory Studies of Water Transport in Rock Salt, SAND79-1519, Sandia National Laboratories, Albuquerque, New Mexico, 1979.

4. Lambert, S. J., Mineralogical Aspects of Fluid Migration in the Salt Block II Experiment, SAND79-2423, Sandia National Laboratories, Albuquerque, New Mexico, May 1980.

5. Acton, R. V., Thermal Conductivity of SE New Mexico Rocksalt and Anhydrite, unpublished Sandia National Laboratories preliminary report, 1977.